Book Chapter for "Sea Ice: An introduction to its physics, biology, chemistry, and geology," David Thomas, Editor, 12-20-01

Large Scale Characteristics and Variability of the Global Sea Ice Cover

Josefino C. Comiso
Laboratory for Hydrospheric Processes, Code 971
NASA Goddard Space Flight Center
Greenbelt, MD 20771

Abstract

More than two decades of satellite passive microwave data are used to study and evaluate the large scale characteristics and the changing state of the sea ice cover in both the Northern and Southern Hemispheres. Satellite data provide day/night almost continuous observation of global sea ice cover thereby enabling quantitative variability studies at various time scales. Despite coarse sensor resolution, spatial detail is provided through the use of sea ice concentrations which are derived using an algorithm that determines the fraction of ice and open water within each satellite footprint. Large seasonal fluctuations in the extent are apparent with those of the Southern Hemisphere having larger amplitudes but less symmetrical seasonal distribution than those of the Northern Hemisphere. The large scale interannual variability of the ice cover has been evaluated globally as well as regionally and in the Northern Hemisphere, the yearly anomaly maps show a predominance of positive values in the 1980s and negative values in the 1990s. Regression analysis show that the ice extent and ice area are on a decline at the rate of $-2.0 \pm 0.5\%$ and $-3.1 \pm 0.3\%$ per decade, respectively, in the Northern Hemisphere but there are regions like the Bering Sea with positive trends. What is intriguing, however, is that the perennial sea ice cover has been declining at a much faster rate than for the entire hemisphere, i.e., $6.7 \pm 2.4\%$ and 8.3 ± 2.4 % per decade for ice extent and ice area, respectively. The perennial ice cover consists mainly of thick multiyear ice floes, and its persistent decline would mean a reduction in the average thickness of sea ice and a change in the overall characteristics of the Arctic sea ice cover. Furthermore, the yearly anomaly patterns are coherent with those of surface temperatures derived from 19 years of thermal infrared AVHRR data. The latter also shows that in consolidated ice regions,

the average temperature during summer minima has been increasing at about 0.9 ± 0.6 K per decade. In the Antarctic, large year to year anomalies in the ice cover are observed but they follow a pattern of alternating positive and negative anomalies around the continent. Similar patterns are observed in the yearly surface ice temperature anomaly maps that together with the ice data show consistency with a propagating Antarctic Circumpolar Wave that circle around Antarctica. Unlike the Arctic, the trend in the Antarctic ice cover is positive at 0.4 ± 0.3 % per decade and basically insignificant. However, the ice cover in the Bellingshausen/Amundsen Seas sector have been declining considerably at -8.1 ± 1.4 % per decade while the adjacent Ross Sea sector has been gaining ice at almost the same (but positive) rate at 7.0 ± 1.0 % per decade. The significance of the trend study results from the relatively short term satellite record is analyzed in terms of longer proxy records and the short term effects of the retreating ice cover is discussed.

1. Introduction

At high latitudes, the global oceans are covered by vast blankets of sea ice which ranges in extent at any one time between 20×10^6 to28×10^6 km^2. The areal extent of the ice cover thus corresponds to a significant fraction (4 to 6%) of the total surface area of the Earth. In the Arctic region, the winter ice cover is about double that of the summer while in the Antarctic, the corresponding value is five-fold (Zwally, et al., 1983; Parkinson et al., 1987; Gloersen et al., 1992). The sea ice cover is thus one of the most expansive and most seasonal geophysical parameter on the Earth's surface, second only to the more variable and less predictable snow cover. The presence or absence of sea ice impacts the atmosphere and the ocean, and therefore the climate, in many ways. For example, as an insulating material, it limits the flow of heat between the ocean and atmosphere. On account of its high albedo, it also keeps a high fraction of solar radiation from being directly absorbed by the surface. Moreover, climate change signals are expected to be amplified in polar regions because of feedback effects associated with the high albedo of ice and snow (Budyco, 1966). The latter has been the subject of many recent investigations, especially in light a declining sea ice cover (Jacobs and Comiso,

1993; Johannessen et al., 1995; Cavalieri et al., 1997; Rothrock et al., 1999; Wadhams and Davis, 2000).

The advance and retreat of sea ice during growth and decay, respectively, cause horizontal and vertical redistributions of salt in the ocean that can profoundly affect the latter. During ice formation, brine rejection causes enhanced salinity of the underlying ocean and this process could initiate vertical convection and/or the formation of bottom water. Conversely, during ice retreat, low salinity melt water is introduced and cause the upper layer of the ocean to be stratified and vertically stable thereby promoting phytoplankton growth and increased productivity in the region (Smith et al., 1988; Comiso et al., 1992; Arrigo, 2002, this volume). Large polynyas within the pack and ice features (e.g., Odden) have been discovered and associated with deep ocean convection (Gordon and Comiso, 1988). Latent heat polynyas near the coastal regions caused primarily by strong katabatic winds have also been observed (Zwally et al., 1985; Comiso and Gordon, 1998; Markus et al., 1998; Massom et al., 1999) and have been postulated as the key source of the high salinity bottom water that is involved in global thermohaline circulation.

The large scale variability of the sea ice cover has been quantified previously using satellite passive microwave data (Zwally et al., 1983; Parkinson et al., 1987; Gloersen et al. 1992; Johannessen et al., 1995; Cavalieri et al., 1997; Stamerjohn and Smith, 1997; Parkinson et al., 1999; Zwally et al., in press). Large changes in the ice cover have been reported in the 1990s, especially in the Arctic, but more detailed studies are needed to better understand the climate system in the region. In this chapter, the current state and variability of the sea ice cover is evaluated using the most up-to-date satellite data available. Although the merit of passive microwave data for sea ice studies have been noted, results from different ice algorithms are not identical (Stamerjohn and Smith, 1997; Comiso et al., 1997; Comiso and Steffen, in press). The ice concentration data used in this study are those derived using the Bootstrap sea ice algorithm that has been chosen as the standard algorithm for new passive microwave satellite systems (i.e., AMSR). The results presented in this chapter update those presented by Stamerjohn and Smith (1997) and Jacobs and Comiso (1997) and can be used for comparative analysis with results from other data sets. Also included are the results of analyses of changes in

environmental forcings, such as temperature, that affect the ice variability and trends in the ice cover.

2. Satellite Observations

Detailed studies of the global sea ice cover are made possible by the advent of satellite data that provide comprehensive areal coverage at a relatively high temporal resolution. When the weather and conditions are right, high resolution visible data, like Landsat and SPOT, provide good and spatially detailed characterization of the ice cover. An excellent example of the utility of such data are the pair of Landsat TM images, shown in Figure 1, that depicts the small scale and large scale physical changes in the ice cover from one season to another. The image in Figure 1a shows typical conditions during early stages of ice growth in the Antarctic, which in this case is located near the Cosmonaut Sea and Cape Ann. During this time period, small platelets and needles called frazil ice are formed in supercooled water and through wave action and wind, the ice particles are accumulated to form shuga and small pancakes. The spatial pattern of the ice cover show a highly dynamic region with the apparent thermodynamic ice growth being accompanied by open water formation caused by wind, waves, tides, and icebergs. The image in Figure 1b was taken in spring, approximately 8 months later, in the same general area. During this latter period, a much thicker ice cover is apparent, large ice floes are well defined and are shown to be composed of a complex conglomerate of various ice types. A spring polynya along the coast is also apparent and may be initiated mainly by ice breakup due to upwelling of warm water and/or advection due to wind. To understand the changes in the ice cover, such seasonality in physical characteristics has to be recognized since the overall effect of the ice cover depends on the latter.

To illustrate the circumpolar nature and general large scale distribution of the sea ice cover during both growth and decay periods, observations from one of the visible channels of AVHRR (Advanced Very High Resolution Radiometer) during the last week of April and November 1989, are presented in Figs. 2a and 2b, respectively. Each of the images represents a weekly average derived from AVHRR Global Area Coverage (GAC) data and mapped into a 6.25 by 6.25 km grid, as described by *Comiso* [2000]. Polynyas, especially near the coastal regions, are shown in the AVHRR images as relatively darker

than the thicker ice cover even when they are already covered by new ice. At the marginal ice zones, the ice cover is also shown to be grayish and sometimes difficult to discriminate from open water. Overall, visible channel images provide good information about regions of high consolidation and areas of divergence or active ice formation.

Passive and active microwave systems have been more popular techniques because of day/night almost all-weather capabilities and global coverage at a relatively high temporal resolution. For large scale variability and trend studies, passive microwave data have an advantage because of relatively long, comprehensive, and consistent historical record. An apparent weakness of passive microwave data is the coarse spatial resolution (about 25 by 25 km) which makes such data difficult to use for detecting small spatial features in the ice cover, such as leads, ridges, and ice bands. To overcome this weakness, algorithms have been applied to obtain needed information (e.g., ice concentration) within each grid element.

The color-coded images in Figures 2c and 2d correspond to sea ice concentrations derived using the Bootstrap Algorithm (Comiso, 1997) for the periods corresponding to those of Figures 2a and 2b, respectively. Overall, there is a good coherence in the images, with the gray areas in the AVHRR satellite image corresponding to the relatively low concentration ice areas depicted in the passive microwave data. The spatial changes in signature look similar in both visible and passive microwave data for the two periods and reflect primarily changes in the physical properties of the ice cover. During the growth period in autumn, large areas in the ice covered region look gray in the AVHRR image because of relatively low reflectivity for new ice (Allison, 1981; Massom, 1991). The same surfaces also have low brightness temperatures and hence relatively low concentration because of low microwave emissivity compared to that of thick ice (Comiso et al., 1992; Grenfell et al., 1994). Conversely, during the breakup period, the gray (low reflectivity) areas (Figure 2b) correspond proportionately to relatively more open water and therefore lower ice concentration as depicted by the corresponding passive microwave data (Figure 2d). Thus, intermediate ice concentration values in the microwave data usually reflect the presence of newly formed ice (as in leads and polynyas) in autumn and winter and the presence of mixtures of ice and open water in spring. Since open water in leads and polynyas are covered by ice of some form within

hours of formation in autumn and winter, this is also a more useful way of quantifying the ice cover compared to a strict ice and no ice discrimination that would show near 100% ice cover in practically all regions during growth stages.

For studies that require high spatial resolution irrespective of weather and time, SAR data which has a resolution of about 35 m can be very useful. Ice floes and ridges are recognizable within the ice pack but in some areas, especially near the ice edge, the interpretation of the data is sometimes not unambiguous. However, with the use of time series of images, some of the ambiguities can be resolved and the drift of sea ice can also be inferred (Kwok et al. 1998). A problem in terms of global coverage is the paucity of data and the lack of sufficient spatial and temporal coverage. The other active microwave system available that provides less resolution but more comprehensive coverage is the scatterometer, an example of which is the QuickSCAT and NSCAT as described by Massom (1991) and Drinkwater (1999). The data coverage and resolution are similar to those from passive microwave but more research is needed to accurately interpret the data and algorithms have to be developed to retrieve geophysical parameters.

3. Spatial and Temporal Variations of the Sea Ice Cover

The physical characteristics and spatial distribution of the global sea ice cover have been discussed extensively in the literature (Weeks and Ackley, 1986; Eicken et al., 1991; Tucker et al., 1992; Eicken, this volume). Because of geographical location and other factors (Figure 3), the distribution of sea ice in the Northern Hemisphere (NH) is quite different from that of the Southern Hemisphere (SH). In the NH, sea ice is surrounded by land with the latter providing an outer limit in the extent of the sea ice cover in most places. In winter, the ice cover in the region is fragmented with the largest fraction in the Arctic region, including the North Pole, and the rest in the Canadian Archipelago and in the peripheral seas as far south as 40° N. In the summer, the ice cover is contiguous and is confined to the Arctic Basin. On the other hand, in the SH, the sea ice cover surrounds the Antarctic continent with the highest latitude being about 80 ° N but there is no limit in the northern regions. In the SH, a contiguous ring of sea ice surrounds the Antarctic continent in winter and is not restricted in its advance towards the north by a land boundary. However, during the end of the summer, the ice cover is

fragmented and located mainly in the Western Weddell Sea, Bellingshausen Sea, and Admunsen Sea and parts of the Ross Sea and the Indian Ocean.

The growth and decay periods of sea ice in the two hemispheres are out of phase by about 6 months because the seasons in the two regions are correspondingly out of phase. In addition, the environmental conditions are different as discussed earlier. The patterns for growth and decay in the two regions are therefore not expected to be identical. Climatological monthly averages derived from 22 years of passive microwave data are shown in Figure 4 and it is clear that the seasonal distributions for the two regions are indeed different. In the NH, there is symmetry in the distribution in that the growth period is approximately as long as the decay period. In the SH, the growth season is significantly longer (by about 2 months) than the decay season.

In the NH, the mean monthly extent (Figure 4a, solid line) is shown to vary from a minimum of 6.2×10^6 km^2 in the late summer (September) to about 15.5 km^2 in the winter (March). The corresponding values in the SH (Figure 4b, solid line) are 3.8×10^6 km^2 (in February) and 19×10^6 km^2 (in September), respectively. Note that although the minimum values in the NH are greater than that in the SH, the effective polar albedo in the latter is much greater than that of the former because of the presence of the snow covered Antarctic continent which has a total area of about 14×10^6 km^2. Thus, interannual changes in summer when the solar insolation is high, is likely more critical in terms of changes in atmospheric forcing since the percentage change in albedo is higher in the NH than in the SH.

In the NH, the monthly values during the year when the winter ice extent is most extensive (i.e., 1979) during the 22 year period are represented by data points connected by dash lines in Figure 4a. It is apparent that the rate of decay during the year when ice is most extensive is less than average and the summer values are also above average. Conversely, the monthly values for the year when the ice is least extensive in winter (i.e., 1996) are shown by the dotted line and it is apparent that the rate of decay is higher than average and with ice extent in summer is considerably less than average. Thus, extensive ice cover (icy) in winter is usually followed by extensive ice cover in summer and vice-versa.

In the SH, the monthly ice extents during the year when the winter was most expansive (1980) or least expansive (1986) are also shown in dash and dotted lines, respectively. It is apparent from the plots that in this hemisphere, the growth and decay patterns are similar to those of the average and are not significantly influenced by the extent of ice during the winter period. Regionally, however, effects opposite to that in the Arctic have been observed. For example, in the Weddell Sea, anomalously extensive ice cover in winter is usually followed by anomalously low ice cover area in the summer (Comiso and Gordon, 1998).

The retreat of sea ice in the Antarctic is more rapid than in the Arctic because in the latter, the ice cover is protected from direct intrusions of warm water from lower latitudes and from breakup by large ocean waves by the presence of surrounding land boundaries, while in the former, there is no such protection. Also, the ice extent reaches its maximum value faster in the Arctic than in the Antarctic likely because of relatively colder environment in the former during autumn and winter since the latter is surrounded by relatively warm oceans. For completeness, the climatological global sea ice cover, which is basically the sum of data in Figures 4a and 4b, is presented in Figure 4c. The plot shows that at any one time, on the average, the ice cover ranges from 19.0 to 27.5 x 10^6 km^2 but the extents can be as low as 17.5 x 10^6 km^2 and as high as 28.5 x 10^6 km^2. While the low values occur in February as expected, the high values apparently occur in November.

The large seasonal variability in the extent (Figure 4) makes it difficult to assess interannual variability from the time series of monthly data. To study interannual changes, seasonal averages for each year are presented in Figure 5 for the period from 1979 to 2000 . The plots for the Northern Hemisphere (Figure 5a) show significant interannual variability during summer and autumn but there were only small changes during winter and spring, especially during the 1990 to 2000 period. The summer averages have higher values than the autumn averages because the latter includes September which is the month of minimum extent. In the Southern Hemisphere, the interannual changes appear minimal for all seasons except for 1980, 1982, and 1997 during summer and autumn. The plots for ice area in both hemispheres (not shown) are similar in characteristics as those for ice extents but the values are significantly lower. In

this case, the summer values are lower than the values during autumn because of relatively lower concentrations during the period.

The dotted lines in the plots in Figure 5 represent the trends in the ice cover for the different seasons as derived from linear regression of all the data points. The trends are all negative in the northern hemisphere and all slightly positive in the southern hemisphere, as has been reported previously, but with slightly different values. This phenomenon suggests that the climates of the two hemispheres are not closely coupled and may be independent of each other. A more detailed discussion of these results will be presented in a later section.

3.1 The Arctic Region

The basic data used for studying the seasonal and the interannual variability of the ice cover are daily averages of ice concentrations mapped onto a polar stereographic grid. The data provide good temporal resolution and are used for calculating monthly-ice entent, monthly-ice area, and monthly-ice concentration for each month from 1979 to 2000, as shown in Figures 6a, 6b, and 6c respectively. The distributions for both ice extent and actual ice area are coherent and show similar patterns. The peak values are also shown to have much less interannual variability than the minimum values, especially in the 1990s. Relatively low values in the minimum ice extent (Figure 6a) are apparent in 1990, 1991, 1993, 1995, 1998, 1999, and 2000. In the ice area plot (Figure 6b), the minimum values during these years appear even relatively lower. This is partly because of relatively lower average concentrations (Figure 6c) which in turn may be partly due to more divergence and/or meltponding during these later years.

The color coded yearly-anomaly maps, presented in Figure 7, provide the means to assess large scale and regional changes in the ice cover on a year to year basis. For uniformity in both hemispheres, yearly averages are calculated by starting from mid-summer through winter and to the following summer. More specifically, in the Northern Hemisphere, the yearly averages are from August of one year to July the following year while in the Southern Hemisphere, it is from January to December the same year. The yearly maps, as defined, represent averages of ice concentrations as the ice cover evolves from growth stages through its maximum values in winter and through melting stages in

spring and summer. Each map in Figure 7 thus represents the anomalies within each ice season instead of within each calendar year. Positive changes in the ice cover are shown in the color coded maps as grays, greens or blues while negative changes are in oranges, purples, and reds.

It is apparent that much of the interannual changes are found in the peripheral seas. Among the most active areas in the Pacific Ocean region are the Sea of Okhotsk and the Bering Sea. Some teleconnections between these two seas have been observed previously (Cavalieri and Parkinson, 1987) with negative changes occurring in one sea while positive changes were occurring in the other sea (e.g., 1979, 2000). The patterns are apparently not consistent since the anomalies can be both negative in these regions, as in 1984 and 1996, or both positives, as in 1980 and 1993. In other years, the patterns are not so clear with a mixture of positives and negatives even in the same seas. In the Atlantic Ocean side, similar effects are also evident between Kara/Barents Seas and Baffin/Hudson Bays. It is interesting to note that there was no year in which the changes are either all positive or all negative in the peripheral seas.

To quantitatively evaluate interannual changes, anomaly plots for the entire hemisphere and various sectors in the Arctic region (as described in Gloersen et al., 1992) are presented in Figure 8 for the 1979 to 2000 period. Each data point in the anomaly plots is the difference of the value for each month and that of the corresponding climatological value (as shown in Figure 4). The use of monthly anomaly plots provides a means to assess interannual variability since the large yearly seasonality is subtracted. Statistically, they also provide better accuracy for trend analysis than yearly or seasonal averages. The anomalies in ice extent and ice area again show coherence and reflect very similar characteristics. It is also apparent, that the abnormally low and high values stands out better in these plots than in the raw monthly plots shown in Figure 6. What stands out most in this plot is the abnormally low value in 1995 followed by abnormally high value in 1996. This is an indication that dramatic changes can occur from one year to another.

In the Arctic sector (Figure 8b), the anomalies are significant only during spring, summer, and autumn since during winter, the entire Arctic basin is covered by ice. It is apparent that the anomalies are all positive in the 1980s and mainly negative in the 1990s,

the exceptions being 1992, 1994 and 1996. The anomalies in the Greenland Sea sector (Figure 8c) show more variability through the 22-year period. A cyclical pattern is apparent in the distribution for this sector mainly as a result of similar changes in the extent of the Odden, as described by Comiso et al. (2001). In the Kara/Barents Seas (Figure 8d) the variability is similar to that of the Greenland Sea but a cyclical pattern is not as apparent. In this sector, significant decreases are apparent in 1983, 1985, 1992, 1995 and 2000 while increases occurred in most other years. The sea ice anomalies in the Bering and Okhotsk Seas (Figures 8e and 8f) have similar variability but opposite trendss with the former having negative anomalies in the 1980s and mainly positive anomalies in the 1990s. In the Okhotsk Sea, the anomalies were on the average positive in the 1980s, except in 1984, and negative in the 1990s, except for the last few years. In the Canadian Archipelago, the anomalies in extent were generally small except for the one big drop in extent in 1998. This was the same year when the Beaufort Sea had the largest open water area during the satellite era. In the Baffin Bay/Labrador Sea region, periodic fluctuations in the anomalies (Figure 8h) are apparent in the 1980s but in the 1990s, except for the recoveries in 1993 and 1996, the extent was generally declining. In the Hudson Bay, there is not much variability except for positive anomalies in 1983, 1986 and 1992 and negative anomalies in 1993, 1994, 1998 and 1999. At the Gulf of St. Lawrence, there is a suggestion of periodicity with all negative anomalies up to 1983 followed by all positive anomalies up to 1993 and then negative anomalies up to the present.

The plots in Figure 8 show that there is no pattern of consistency in the variability of the ice cover in the different sectors. The peaks and the dips generally do not occur at the same time in the different regions and periodicities, where they occur, are usually out of phase from each other. This is partly because the ice cover is partly controlled by a complex atmospheric system that produces different ice distributions in the different regions during different periods. The effect of surface temperature anomalies will be discussed in a later section. Overall, negative trends of varying degree of significance are observed in all sectors, except for the Bering Sea sector in which the ice cover have been increasing at the rate of 11.9%/decade.

3.2 The Antarctic Region

Monthly ice extents, ice area, and ice concentration in the Southern Hemisphere for the period from 1979 through 2000 are presented in Figure 9, and it is apparent that there are differences in the distributions compared to those in the Northern Hemisphere. In the SH, the amplitude of each ice season is obviously larger while the yearly distributions are more regular than those in the NH. The average ice concentration is almost constant at about 83% in winter, compared to about 92% in the Arctic, while the average ice concentration in the summer ranging from 59% to 69%, compared to 72 to 81% in the Arctic. Note that the distributions for ice extents are again coherent with those of ice area with the latter being lower in values, as expected.

Color coded anomaly maps for each year from 1979 through 2000, as shown in Figure 10, illustrate the large year-to-year variability in the ice cover in the region. The images shows patterns of alternate negative and positive anomalies at the periphery of the sea ice cover around the continent. From one year to another, these patterns tend to move around propagating like a wave, as described by White and Peterson (1996). The period of propagation has been inferred as about 8 years with a revisit time of 4 years at every point since the wave number is mode 2. It is interesting to note that the pattern of anomalies in 1980 is almost duplicated in 1992. Also, the anomaly pattern in 1999 is almost identical to that of 1980 but with opposite sign. The repetition of the patterns in some places suggests that there are local geographic or oceanographic factors that cause similar features to be reproduced in different years.

The plots of monthly ice extent anomalies for the entire hemisphere, as well as in various sectors (see Gloersen et al.,1992), as shown in Figure 11, are indicative of a very variable and dynamic region. The anomalies for the entire hemisphere (Figure 11a) apparently have higher amplitudes in the 1980s than in the 1990s but the same phenomenon is not evident in the various sectors. The peaks and dips in the anomaly plots are again shown to occur in different years in the various sectors. This is partly because of the propagating wave (ACW), which as described earlier, causes the anomalies to circle around the continent. But again, the patterns are relatively unpredictable since the climate system in the region is complex and driven by many other factors, some of which are regional. In the Weddell Sea sector, a positive anomaly in

1981 was followed by a negative anomaly in the subsequent summer while a negative anomaly in 1991 was followed by two years of positive anomalies. In the Indian Ocean sector, negative anomalies in 1987 and 1988 were followed by positive anomalies in 1989 and 1990. In the Western Pacific Ocean sector, the key events were the positive anomalies in 1982 and 1983 and the negative anomaly in 1989. In the Ross Sea, a large negative anomaly in the early 1980s was followed by positive anomalies except for slight drops in 1991 and 1997. In the Bellingshausen/Amundsen Sea sector, the years of 1983, 1988, 1992, and 1998 are shown to be associated with low negative anomalies suggesting some association of this region with ENSO events which occurred during the same period (Peterson and White, 1997; Kwok and Comiso, 2001). Note that the dips at the Ross Sea sector (i.e., 1980, 1986, 1992, 1995, and 1997) which is also regarded as a site affected by ENSO (Ledley and Huang et al., 1997) are not coincident with those of the Bellingshausen/ Amundsen Sea sector.

4. Global and Regional Trends

Global climate change is expected to be amplified in the polar regions because of enhanced feedback effects associated with the high albedo of ice (Budyco, 1976) as indicate earlier. Significant changes in the sea ice cover have already been reported (Johannessen et al., 1995; Cavalieri et al., 1997; Rothrock et al., 1999; Wadhams et al., 2000; Tucker et al., 2001). Since a global warming of 0.5 K has been observed during the last century (Jones et al., 1999), it is important that this phenomenon is studied in greater detail. Linear trend analyses have been applied on the monthly sea ice anomalies from 1979 through 2000 and results are shown as dotted line in Figures 8 and 11. The values are also tabulated in Tables 1 and Tables 2 for the Northern and Southern Hemispheres, respectively.

The trend in ice extent in the Northern Hemisphere as inferred from monthly anomaly data from January 1979 through December 2000 is -2.0 ± 0.3 % per decade. This is less than the rate of -3 %/decade inferred previously from slightly different data sets for the years November 1978 to December 1996 (Johannessen et al., 1995; Cavalieri et al., 1997) and November 1978 to December 1998 (Parkinson et al, 1999). With the data set used in this study, the trend for the 1978 to 1998 period is 2.8 ± 0.4x %, per

decade which is consistent with the other reported values. It is thus important to note that significant changes in the trend can happen as more data are compiled, especially if the latest values are very different from previous ones. The issue of accuracy associated with record lengths of data is addressed in the next section.

In the Central Arctic region, the trend is -1.2 ± 0.2 % per decade, which is a lesser negative rate than that for the entire Northern Hemisphere. The lesser rate is not unexpected since much of the anomalies are in the peripheral seas as discussed in the previous sections. The plot in Figure 8b indicates spikes associated with changes in the spring and summer periods which are shown to be mainly positive in the 1980s and negative (except for 1992, 1994, and 1996) in the 1990s. The negative trend appears to be primarily influenced by unusually low ice extent events of 1990, 1993, and 1995.

The trends in other sectors are varied with the only positive trend occurring in the Bering Sea at 11.9 ± 2.6 % per decade. This reflects increases in the winter ice cover in the region despite decreases in the ice cover in the adjacent (Arctic) region. Also, towards the southwest of this region at the Okhotsk Sea, the ice cover is declining at about the same magnitude but opposite sign with the trend being -11.0 ± 2.7 % per decade. In the latter, the trend would have been significantly more negative were it not for the relatively strong recovery during the last two years of data. Other regions with significant negative trends are the Kara/Barents Seas and Hudson Bay with trends of -5.5 ± 1.2 % per decade and -4.5 ± 1.0 % per decade respectively. The trend at the Canadian Archipelago is also significant at -1.9 ± 0.4 % per decade but this is mainly due to a big drop in ice cover in the region in 1998. Trends are also negative in the Greenland Sea and Baffin Bay/Labrador Sea sectors at -2.7 ± 1.3 and -1.3 ± 1.4 % per decade, respectively, but changes in these regions may be partly influenced by periodic patterns as mentioned previously. A periodic pattern is also evident at the Gulf of St. Lawrence sector which show an insignificant trend of -0.5 ± 5.0 % per decade.

While the trend of ice cover in the entire Northern Hemisphere is basically controlled by trends in the peripheral seas, the most important trend of interest is actually that associated with the Central Arctic. The Northern Hemisphere has smaller seasonal amplitude than the Southern Hemisphere because of the presence of extensive and thick multiyear ice cover in the Central Arctic. Ice that survives the summer is often referred

to as the perennial ice cover, which consists mainly of multiyear ice. The extent and area of the perennial ice cover can be inferred by finding the minimum value for each year from time series. The yearly record of the minimum extents of the ice cover for each year from 1979 to 2000 is shown together with that of maximum extent in Figure 12. The trends in maximum ice values for both extent and ice area are -1.33 ± 0.59, and -1.85 ± 0.58, respectively, and are basically consistent with those of the entire hemisphere (Figure 12a). The trends in minimum ice cover, however, are -6.37 ± 2.13 %/decade and -8.49 ± 1.98 %/decade for ice extent and ice area, respectively (Figure 12b). Such large negative trends (about 4 times higher than maximum trends) indicate that the perennial ice cover consisting mainly of multiyear ice floes is shrinking at a very high rate. Similar results have been reported previously for a shorter time period (Comiso, 2001, in press). Trends of similar magnitude has also been reported by Johannessen et al. (1999) using multiyear ice fraction data derived during winter period from passive microwave data. However, such data are known to have large uncertainties (Kwok et al., 1996) partly because the emissivity of multiyear ice is highly variable and not constant as assumed by the multiyear ice algorithm.

Of special interest in the plot shown in Figure 12b is the large yearly variability of summer sea ice in the 1990s compared to the 1980s. As reported in Comiso (2001, in press) such variability suggests an increasing concentration of second year ice cover in the 1990s, compared to those in the 1980s, and in effect a thinning of the Arctic sea ice cover (that includes the second year ice cover). This is consistent with reports by Rothrock et al. (1999) and Wadhams and Davis (2001) that the average ice thickness in the 1990s is significantly less that that collected in th previous decades. It would be of interest to know if much of the thinning is associated with this phenomenon. The issue of change in thickness is addressed in a separate chapter (Hass, this volume).

On a season by season basis, the interannual trends have been shown previously in Figure 5. The numerical values of the trends are given in Tables 1 and 2. In the Northern Hemisphere, it is apparent that the trends are all negative with those for winter and spring being only slightly negative at -0.75 ± 0.55 %/decade and -1.25 ± 0.48 % per decade, respectively. In the autumn, the trend is more negative at -2.69 ± 1.27 %/decade but it is the summer that has a high rate of decrease, at -4.12 ± 0.90%/decade. The latter

is consistent with the large rate of decrease for the perennial ice cover. An even higher rate of decrease is observed when ice area data are used with the rate of decrease during the summer being as low as –6.04 ± 1.09 %/decade.

The trend results in the Southern Hemisphere (Figure 11) are not as indicative of a changing ice cover as those of the Northern Hemisphere. The result of analysis of data from the 22-year period shows an insignificant trend of 0.4 ± 0.3 % per decade for the entire Southern Hemisphere. The trends are similarly insignificant at –1.2 ± 0.8, 0.1 ± 0.9, and 1.2 ± 1.2 % per decade at the Weddell Sea, Indian Ocean, and Western Pacific sectors, respectively. In two other sectors, however, the changes are quite strong with opposite trends of 7.0 ± 1.0 % per decade and –8.1± 1.4 % per decade at the Ross Sea and Bellingshausen/Amundsen Seas sectors, respectively. Since the two sectors are adjacent to each other, it appears that the opposite trends in the two sectors are partly caused by advection of ice from one sector to the other. However, the Antarctic Penninsula that is adjacent to the B/A sector has been an area of climate anomaly as described previously by Jacobs and Comiso (1997) and King (1994). Also, the Ross Sea region has been associated with influences of ENSO (Ledley and Huang, 1997) and the continental area adjacent to it has been experiencing some cooling during the last two decades (Comiso, 2000). The trend in the Ross Sea, which is the site of some of the major coastal polynyas, suggests that the role of the region in bottom water formation is becoming more important.

The trends of maximum ice values for each year in the Southern Hemisphere is again similar to that inferred from the monthly time series, being 0.28 ± 0.54 % per decade and 1.20 ± 0.58 % per decade for ice extent and ice area, respectively. It is, however, surprising that the trends of minimum values for each year are negative at –3.58 ± 2.83 and –3.76 ± 3.16 for ice extent and ice area, respectively. It appears that the summer ice cover has been declining as in the Arctic but errors are larger because of much lower extent of ice in the summer.

In the Southern Hemisphere, the trends for extent in each season (Figure 5b) are basically insignificant except for autumn. Quantitatively, in winter, spring, and summer, the trends are 0.52 ± 0.56, -0.08 ± 0.54, -1.78 ± 1.77, respectively, while in autumn, a positive and significant trend of 3.20 ± 1.70 is inferred. It is apparent that the net positive

trend for all seasons is caused mainly by changes in autumn. Again, the trend for ice area is higher than those for ice extent, with that for autumn being 5.46 ± 2.00 while those for winter, spring, and summer, being 1.47 ± 0.62, 0.78 ± 0.66, and 0.21 ± 1.95, respectively. The higher positive trend in autumn suggests that the onset of ice growth may be occurring earlier and earlier during the latter part of the study period. Also, the negative (though insignificant) trends in spring and summer may indicate earlier breakup in the latter part of the data set as well.

5. Surface Temperature Effects, Temperature Trends, and Cyclical patterns

To gain insights into the observed variability and trend in the ice cover, we examine the anomalies in the ice cover in conjunction with anomalies in surface temperatures. Surface temperatures are used because they are known to be negatively correlated with ice extent and area (Jacobs and Comiso, 1997). However, it should be pointed out that changes in pressure and other parameters are also important (Walsh et al., 1999) but the effect of pressure is a lot more complex and is not within the scope of this chapter. Following Comiso (2000) and Comiso (2001), the anomalies in yearly surface temperatures as derived from AVHRR data for the Northern and Southern Hemispheres are shown in Figures 14 and 15, respectively. The last image in each figure is the climatological yearly data that is used in generating the anomaly maps.

It is remarkable that the temperature anomaly maps in the Northern Hemisphere show generally negative anomalies (greens and blues) in the 1980s and positive anomalies in the 1990s. This alone is indicative of warming during the last two decades. This phenomenon is also consistent with a declining sea ice cover in the Arctic as shown previously. It should be noted, however, that there are areas of positive anomalies in the first decade of data, such as the Greenland/Baffin Sea area in 1981-1982 and the Kara/Barents Sea area in 1983-1984. Conversely, there are also negative anomalies in the second decade such as in the Canadian Archipelago/Beaufort Sea area in 1990-1991 and the Kara/Barents Sea area in 1998-1999. This indicates that while temperature is increasing in most parts of the Northern Hemisphere, there are areas in which temperature have been decreasing.

The areas of positive anomalies in surface temperature are shown to be precisely where negative anomalies in the sea ice cover (Figure 7) are observed. Although there are many other factors, such as wind, upwelling and tides, that affect the sea ice distribution, the good coherence with temperature is an indication that warming plays a big influence on the observed changes in the ice cover. There is also a feedback effect in that as the perennial sea ice cover declines and open water area increases in the Arctic Basin in spring and summer, more solar energy and heat are absorbed by the Arctic ocean. This in turn warms up the latter and cause a further decline in the ice cover. Some evidence that the temperature of the Arctic Ocean has been increasing has in fact been reported (Gunn and Muench, 1999).

The yearly temperature anomaly maps in the Southern Hemisphere (Figure 15) do not exhibit the same warming trend observed in the Northern Hemisphere. What is of great interest, however, is the presence of alternating negative and positive anomalies around the continent, especially at the ice edges. Such anomalies are again coherent with the sea ice cover anomalies in Figure 10. Note that the temperature anomalies beyond the sea ice covered regions (i.e., those of the open ocean and the continent), are also coherent with those observed over sea ice (Figure 10). It is apparent that the influence of the Antarctic Circumpolar Wave is not just an ice edge phenomenon as previously thought (White and Peterson, 1996). The anomaly patterns also indicate that atmospheric effects play an important role in the variability of the sea ice cover.

Because of the high correlation of the ice cover with surface temperature, long historical data from meteorological stations (Jones et al., 1999) in the Northern and Southern Hemispheres were studied and results are presented in Figures 16 and 17. It is apparent that the length of a data record can make a big difference when trend analysis is being conducted. Three record lengths of surface temperatures were analyzed, namely, 98, 45, and 20 years. In the NH, the results of trend analysis for data from stations located $>50^{\circ}$ N yielded 0.08 ± 0.01, 0.22 ± 0.04, and 0.38 ± 0.12 K/decade, for the 98, 45, and 20 year time records, respectively (Figures 16a,16b,& 16c). The much higher rate for the shorter time period suggests that the rate of warming may be accelerating. However, if the long term station data set is used to study the sensitivity of the trend values to record length (Figure 16d), it is apparent care needs to be exercised when doing

interpretation of short term data sets. The trend follows a highly fluctuating value in the first 15 years, then a relatively variable value in the next 15 years and then an exponential decline from 1968 to 1900. The plot shows that the 22 year satellite data set may provide useful information but 30 years of data would be more desirable.

Cyclical patterns also need to be considered, specially those associated with the North Atlantic and the Arctic Oscillation (Mysak, 1999; Polyakov et al., 1999). Changes in pressure fields such as those that cause wind and ice motion to go from cyclonic to anticyclonic mode, and vice versa, cause a redistribution of the ice cover and yielding ice anomalies in some areas (Proshutinsky and Johnson, 1997). The temperature data was also analyzed for periodic changes and the result is shown in Figure 15e. Some peaks in the power spectrum have been identified as 12.3, 7, 5.4, and 4.5 years. Trend studies that make use of data with record lengths of similar magnitude as the periods in these cycles may not yield meaningful results.

In the Southern Hemisphere, the trend results are also different for the three periods being 0.03 ± 0.01, 0.10 ± 0.02, and -0.003 ± 0.087 K/decade for the 98-, 45-, and 20-years, respectively (Figure 17a, b, c). While the 45-year trend is more positive than the 98-year trend, as in the Arctic, the 20-year trend came out a slight negative. A look at the running trend as plotted in Figure 17d indicates that the trend actually goes up from a negative value in 1983 (for the trend from 1983 to 1998) to a peak value in 1958 and from there, it became almost stable but declines almost linearly to the 98-year trend. This is intriguing since the observed trend in the 22 year satellite data is consistent with a slightly positive trend in the ice data while the 45-year positive trend is consistent with a decline in the ice cover from the 1950s and 1960s to the present as inferred from ship and whaling data sets (de la Mare, 1997). This indicates that ship and whaling observations may have some value for trend studies despite the inadequacies in the spatial and temporal coverage.

6. Summary and Conclusions

The large scale characteristics of the sea ice cover in the Northern and Southern Hemisphere have been studied using more than two decades of satellite passive microwave and infrared data. High resolution satellite data shows that the sea ice cover

undergoes dramatic changes in its physical characteristics from one season to another. This is detected by passive microwave data as well, through a reduction in ice concentration to compensate for the lower microwave emissivity of new ice compared to that of thick ice. The detection of such areas with dominant new ice cover, including polynyas and ice edges, provide the means to better quantify heat and salinity fluxes over ice covered regions.

The large scale interannual variability of the ice cover has been evaluated globally as well as regionally. Globally, the sea ice cover is shown to be on a decline in the Northern Hemisphere while only minimal change is observed in the Southern Hemisphere. In the Arctic, the rate of decline in extent is strongest in the summer at -4.12 ± 0.90 %/decade and weakest in the winter at -0.75 ± 0.55 %/decade. The rate of decline of the perennial ice cover is even larger at 6.5 and 8.4% per decade for ice extent and ice area, respectively. Such result is important in that the perennial ice cover consists mainly of the thick multiyear ice cover that basically controls the thickness distribution and the limit of sea ice retreat in the summer. A persistent decline in the perennial ice cover at the same rate occurs, profound changes in the Arctic Ocean will occur in the foreseeable future.

In the Southern Hemisphere, the sea ice cover is highly variable but the predictability depends on how well the processes in the region are understood. Alternating negative and positive anomalies occur around the periphery of the ice covered region and year to year changes confirm the presence of an Antarctic Circumpolar Wave that propagates in a clockwise direction about the continent. Both ice and temperature anomalies are highly correlated indicating that these two parameters are indeed closely linked to each other. The year to year changes, however, is not clear-cut and sometimes the anomaly signal from the ACW is difficult to detect.

In a scenario of global warming, it is anticipated that the trend results from Arctic and the Antarctic regions would be similar. However, in the Antarctic region, regression analysis yielded an insignificant positive trend of 0.4 ± 0.3 /decade compared to significant decline in the Arctic as indicated earlier. The yearly anomaly maps in the region, however, show interesting patterns, including some cooling at the pheriphery of the continent. Trend analysis results show that the ice is actually declining at a fast rate

of –8.0 %/decade in the Bellingshausen/Amundsen Seas sector while the adjacent Ross Sea sector has been gaining ice at an equally fast (but opposite) trend. The correlation of ENSO indices with climate anomalies in these regions from a previous study (Kwok and Comiso, in press) was found to be high with the correlation values being of opposite signs for the two regions. The positive trend in the Ross Sea ice cover also suggests a more important role of the Ross Sea region as a source of global bottom water.

Because of the high correlation of ice extent with temperature, we took advantage of the availability of historical meteorological data to study the significance of the satellite results. An analysis of trends as a function of record length shows that the trend results do not become stable until after 20 to 30 years. Since the satellite record is only about this length, interpretation of data should be done with extreme care. Interpretation of trends should also be done in the context of observed cyclic patterns which affects ability to accurately predict future behavior of the sea ice cover. The longer data set also show less negative trend for the Arctic and a slightly negative trend for the Antarctic. This may mean that the satellite observed trends in the Arctic and the Antarctic may be short term, but because of the paucity of meteorological data, and the complexity of climate processes in the region, it is difficult to make definitive conclusions at the present time. With the advent of more sophisticated climate models and more detailed observations from new satellite systems, current assessments of the state of the Global sea ice cover will only improve.

Acknowledgments:

The author is grateful to Rob Gersten and Larry Stocks for excellent programming support. This work was supported by NASAs Cryospheric Process Program and the Earth Science Enterprise.

References:

Ackley, S.F., M. Lange, and P. Wadhams, Snow cover effects on the Antarctic sea ice thickness, Sea Ice Properties and Processes, ed. by S.F. Ackley and W.F. Weeks, *CRREL Monograph 90-1*, 300 pp., Cold Regions Research and Engineering Laboratory, Hanover, New Hampshire, 1990.

Allison, I., Antarctic sea ice growth and oceanic heat flux, Sea Level, Ice and Climatic Change, *International Association of Hydrological Sciences*, Guildfold, UK, pp. 161-170, 1981.

Arrigo, K., Primary production in sea ice, (this volume).

Bjørgo, E., O.M. Johannessen, and M.W. Miles, Analysis of merged SSMR-SSMI time series of Arctic and Antarctic sea ice parameters 1978-1995. *Geophys. Res. Lett.*, 24(4), 413-416, 1997.

Budyko, M.I., Polar ice and climate, In *Proceedings of the Symposium on the Arctic Heat Budget and Atmospheric Circulation*, ed. By J.O. Fletcher, RM 5233-NSF, Rand Corposration, Santa Monica, CA, 3-32, 1966.

Cavalieri, D.J., and C.L. Parkinson, On the relationship between atmospheric circulation and the fluctuations in the sea ice extents of the Bering and Okhotsk seas, *J. Geophys. Res., 92*(C7), 7141-7162, 1987.

Cavalieri, D.J., P. Gloersen, C. Parkinson, J. Comiso, and H.J. Zwally, Observed Hemispheric asymmetry in global sea ice changes, *Science, 278*(7), 1104-1106,1997.

Comiso, J.C., Variability and trends in Antarctic surface temperatures from in situ and satellite infrared measurements, *J. Climate, 13*(10), 1674-1696, 2000.

Comiso, J.C., Correlation and Trend Studies of the Sea Ice Cover and Surface Temperatures in the Arctic, *Annals of Glaciology*, 34 (in press, 2001).

Comiso, J.C., and A.L. Gordon, Interannual variabilities of summer ice minimum, coastal polynyas, and bottom water formation in the Weddell Sea, in Antarctic sea ice physical properties and processes, *AGU Antarctic Research Series Volume 74,* edited by M. Jeffries, 293-315, 1998.

Comiso, J.C., and K. Steffen, Studies of Antarctic sea ice concentrations from satellite data and their applications, *J. Geophys. Res., 106*(C12), 31362-31367, 2001.

Comiso, J.C., D. Cavalieri, C. Parkinson, and P. Gloersen, Passive microwave algorithms for sea ice concentrations, *Remote Sensing of the Env., 60*(3), 357-384, 1997.

Comiso, J.C., P. Wadhams, L.T. Pedersen, and R. Gersten, The seasonal and interannual variability of the Odden and a study of environmental effects, *J. Geophys. Res., 106*(C5), 9093-9116, 2001.

Comiso, J.C, T.C. Grenfell, M. Lange, A. Lohanick, R. Moore, and P. Wadhams,

Microwave remote sensing of the Southern Ocean Ice Cover, Chapter 12, *Microwave Remote Sensing of Sea Ice*, (ed. by Frank Carsey), Am. Geophys. Union, Washington, D.C., 243-259, 1992.

De la Mare, W.K., Abrupt mid-twentieth-century decline in Antarctic sea ice extent from whaling records, *Nature, 389*, 57-60, 1998

Eicken, H., From the microscopic to the macroscopic: Growth, microstructure and properties of sea ice (This volume).

Eicken, H., M.A. Lange, and G.S. Dieckmann, Spatial variability of sea-ice properties in the Northwestern Weddell Sea, *J. Geophys. Res., 96*, 10603-10615, 1991.

Gordon, A. L., and J. C. Comiso, Polynyas in the Southern Ocean, *Scientific American, 256,* 90-97, 1988.

Gloersen P., W. Campbell, D. Cavalieri, J. Comiso, C. Parkinson, H.J. Zwally, Arctic and Antarctic Sea Ice, 1978-1987: Satellite Passive Microwave Observations and Analysis, *NASA Spec. Publ. 511*, 1992.

Grenfell, T.C, D.J. Cavalieri, J.C. Comiso, M.R. Drinkwater, R.G. Onstott, I. Rubinstein, K. Steffen, I. Rubinstein, D.P. Winebrenner, "Microwave signatures of new and young ice," Chapter 14, *Microwave Remote Sensing of Sea Ice,* (ed. by Frank Carsey), American Geophysical Union, Washington, D.C., 291-301, 1992.

Grenfell, T.C., J.C. Comiso, M.A. Lange, H. Eicken, and M.R. Wenshahan, Passive microwave observations of the Weddell Sea during austral winter and early spring, *J. Geophys, Res., 99*(C5), 9995-10,010, 1994.

Gunn, J.T., and R.D. Muench, Observed changes in Arctic Ocean temperature structure over the past half decade, *Geophys. Res. Lett., 28*(6), 1035-1038, 2001.

Hanna, E., Anomalous peak in Antarctic sea-ice area, winter 1998, *Geophys. Res. Lett., 28*(8), 1595-1598, 2001.

Hass, C. , Dynamics versus thermodynamics: The sea ice thickness distribution (this volume).

Jacobs, S.S, and J.C. Comiso, A recent sea-ice retreat west of the Antarctic Peninsula, *Geophys. Res. Lett., 20*(12), 1171-1174, 1993.

Jeffries, M.O., S. Li, R.A. Jana, H.R. Krouse, and B.Hurst-Cushing, Late winter first-year ice flow thickness variability, seawater flooding and snow ice formation in the Amundsen and Ross Sea, in *Antarctic Sea Ice*, ed. M.O. Jeffries, AGU, Washington DC, 69-87, 1998.

Johannessen, O.M., W. Miles, E. Bjorgo, The Arctic's shrinking sea ice, *Nature, 376*, 126-127, 1995

Johannessen, O.M., E.V. Shalina and M.W. Miles, Satellite evidence for an Arctic sea ice cover in transformation, *Science, 286*, 1937-1939, 1999.

Jones, P.D., M. New, D.E. Parker, S. Martin, and I.G. Rigor, Surface air temperature and its changes over the past150 years, *Rev. Geophys., 37*, 173-199, 1999.

King, J.C., Recent climate variability in the vicinity of the Antarctic peninsula, *Int. J. Climatol., 14*, 357-369, 1994.

Kwok, R., and J.C. Comiso, Southern ocean climate and sea ice anomalies associated with the Southern Oscillation, *J. Climate* (in press, 2001).

Kwok, R., J.C. Comiso, and G. Cunningham, Seasonal characteristics of the perennial ice cover of the Beaufort Sea, *J. Geophys. Res.,101*(C2), 28417-28439, 1996.

Kwok R., A. Schweiger, D.A. Rothrock, S. Pang, and C. Kottmeier, Sea ice motion from satellite passive microwave imagery assessed with ERS SAR and buoy motions, *J. Geophys. Res., 103*(C4), 8191-8214, 1998.

Ledley, T.S., and Z.Huang, A possible ENSO signal in the Ross Sea, *Geophys. Res. Lett., 24*(24), 3253-3256, 1997.

Markus, T., C. Kottmeier, and E. Fahrback, Ice formation in coastal polynyas in the Weddell Sea and their impact on oceanic salinity, in Antarctic Sea Ice: Physical Processes, Interactions and Variability, *AGU Antarctic Research Series Volume 74,* edited by M. Jeffries, 273-291, 1998.

Massom, R.A., Satellite Remote Sensing of Polar Regions, Bellhaven Press, 307pp., 1991.

Massom, R.A., J.C. Comiso, A.P. Worby, V. Lytle, and L. Stock, Satellite and in situ observations of regional classes of sea ice cover in the East Antarctic pack in winter, *Remote Sensing of the Env., 68*(1), 61-76, 1999.

Maykut, G. A., Energy exchange over young sea ice in the Central Arctic, *J. Geophy.*

Res., 83(C7), 3646-3658, 1978.

Mysak, L.A., 1. Interdecadal variability at northern high latitutes, In, *Beyond El Nino: Decadal and Interdecadal Climate Variability*, edited by A. Navarra, Springer-Verlag, pp. 1-24, 1999.

Parkinson, C. L., J. C. Comiso, H. J. Zwally, D. J. Cavalieri, P. Gloersen, and W. J. Campbell, Arctic Sea Ice 1973-1976 from Satellite Passive Microwave Observations, *NASA Spec. Publ. 489*, 1987.

Parkinson, C.L., D.J Cavalieri, P. Gloersen, H.J. Zwally, and J.C. Comiso, Arctic Sea ice extents, areas, and trends, 1978-1996, *J. Geophys. Res., 104*(C9), 20837-20856, 1999.

Proshutinsky, A.Y., and M.A. Johnson, Two circulation regimes of the wind-driven Arctic Ocean, *J. Geophys. Res., 102*, 12,493-12,514, 1997.

Polyakov, I.V., A.Y. Proshutinsky, and M.A. Jackson, Seasonal cycles in two regimes of Arctic climate, *J. Geophys. Res., 104*(C11), 25761-25788, 1999.

Rothrock, D. A., Y. Yu, and G. A. Maykut, Thinning of the Arctic sea-ice cover, *Geophys. Res. Lett., 26*(23), 3469-3472, 1999.

Smith, W. O., N. K. Keene, and J. C. Comiso, Potential interannual variability in primary productivity of the Antarctic Marginal Ice Zone, in *Antarctic Ocean and Resources Variability*, ed. by D. Sahrhage Springer, New York, 131-139, 1988.

Stammerjohn and Smith, Opposing southern ocean climate patterns as revealed by trends in regional sea ice coverage, *Climatic Change, 37*, 617-639, 1997.

Steffen, K., Energy flux density estimation over sea ice based on satellite passive microwave measurements, *Ann. Glaciology, 15*, 178-183, 1991.

Tucker III, W.B., J.W. Weatherly, D.T. Eppler, D. Farmer, and D.L. Bentley, Evidence for the rapid thinning of sea ice in the western Arctic Ocean at the end of the 1980s, *Geophys. Res. Lett., 28*(14), 2851-2854, 2001.

Tucker III, W.B., D.K. Perovich, A.J. Gow, W.F. Weeks, and M.R. Drinkwater, Physical properties of sea ice relevant to remote sensing, Chapter 2, *Microwave Remote Sensing of Sea Ice*, (ed. by Frank Carsey), American Geophys. Union, Washington, DC., 201-231, 1992.

Wadhams, P., and N. Davis, Further evidence of ice thinning in the Arctic Ocean,

Geophy. Res. Lett., 27(24), 3973-3976, 2000.

Wadhams, P., M.A. Lange, and S.F. Ackley, The ice thickness distribution across the Atlantic sector of the Antarctic Ocean in midwinter, *J. Geophys. Res., 92*(C13), 14,535-14,552, 1987.

Walsh, J.E., W.L. Chapman and T.L. Shy, Recent decrease of sea level pressure in the Central Arctic, *J. Climate, 9*, 480-486, 1996.

Watkins, A.B, and I. Simmonds, Current trends in Antarctic sea ice: the 1990s impact on short climatology, *J. Climate, 13*, 4441-4451, 2000.

Weeks, W.F., and S.F. Ackley, The growth, structure, and properties of sea ice, in *The Geophysics of Sea Ice,* ed. by N. Unterstiener, pp. 9-164, NATO ASI Series B: Physics vol. 146, Plenum Press, New York, 1986.

White, W.B., and R.G. Peterson, An Antarctic circumpolar wave in surface pressure, wind, temperature, and sea ice extent, *Nature, 380*, 699-702, 1996.

Zwally, H. J., J. C. Comiso, and A. L. Gordon, Antarctic Offshore Leads and Polynyas and Oceanographic Effects, in *Oceanology of the Antarctic Continental Shelf*, ed. by S. Jacobs, Antarctic Research Volume 43, pp. 203-226, 1985.

Zwally, H. J., J. C. Comiso, C. L. Parkinson, W. J. Campbell, F. D. Carsey, and P. Gloersen, Antarctic Sea Ice 1973-1976 from Satellite Passive Microwave Observations, *NASA Spec. Publ. 459*, 1983.

Zwally, H.J., J.C. Comiso, C. Parkinson, D. Cavalieri, P. Gloersen, Variability of the Antarctic Sea Ice Cover, *J. Geophys. Res.* (in press, 2001).

List of Figures:

12. (a) Yearly maximum and (b) yearly minimum of ice extents and ice cover areas in the Northern Hemisphere.
13. (a) Yearly maximum and (b) yearly minimum of ice extents and ice cover areas in the Southern Hemisphere.
14. Yearly surface temperature anomalies in the Northern Hemisphere from 1981 through 2000. Yearly average is derived using data from August of one year to July of the following year.
15. Yearly surface temperature anomalies in the Southern Hemisphere from 1982 through 2000. Yearly average is derived using data from January to December of each year.
16. One-year running mean of surface air temperatures in the Northern Hemisphere for stations located at latitudes >50oN for the period (a) 1978 to 1998; (b) 1950 1998; and (c) 1900 to 1998. (d) trends versus record length starting with the year 1998. (e) Power spectrum using one-year running average data
17. One-year running mean of surface air temperatures in the Southern Hemisphere for stations located at latitudes >50oS for the period (a) 1978 to 1998; (b) 1950 1998; and (c) 1900 to 1998. (d) trends versus record length starting with the year 1998. (e) Power spectrum using one-year running average data.

Table 1. Trends in the Northern Hemisphere

Sector/season	Trend (extent) km^2/dec(%/dec)	Error (extent) km^2/dec (%/dec)	Trend (area) km^2/dec(%/dec)	Error (area) km^2/dec (%/dec)
N. Hemisphere	-24120 (-2.0)	3100 (0.5)	-35080 (3.1)	2800 (0.3)
Arctic Ocean	-7910 (-1.2)	1650 (0.2)	-11570 (-1.8)	1780 (0.3)
Greenland Sea	-1950 (-2.7)	973 (1.3)	-2380 (-4.4)	770 (1.4)
Kara/Barents Sea	-7510 (-5.5)	1600 (1.2)	-8340 (-7.2)	1470 (1.3)
Bering Sea	3760 (11.9)	815 (2.6)	2560 (10.9)	1020 (3.3)
Okhotsk/Japan Sea	-4410 (-11.0)	1080 (2.7)	-5200 (-17.1)	1020 (3.3)
Canadian Arch.	-1360 (-1.9)	284 (0.4)	-2540 (-4.0)	352 (0.5)
Baffin Bay/ Labrador Sea	-1070 (-1.3)	1220 (1.4)	-1670 (-2.4)	1060 (1.5)
Hudson Bay	3570 (-4.5)	820 (1.0)	-3850 (-5.3)	695 (1.0)
Gulf of St Lawrence	-32.9 (-0.5)	357 (5.0)	-91.6 (-2.0)	256 (5.6)
Winter	-10800 (-0.75)	7940(0.52)	-20700 (-1.56)	6820 (0.52)
Spring	-18270 (-1.25)	6990 (0.48)	-27840 (-2.09)	6530 (0.49)
Summer	-42200 (-4.12)	9200 (0.90)	-51350 (-6.04)	9290 (1.09)
Autumn	-24630 (-2.69)	11700 (1.27)	-32220 (-3.94)	10220 (1.25)
Maximum	-21010 (-1.34)	9220 (0.59)	-26870 (-1.86)	8370 (0.58)
Minimum	-45890 (-6.38)	15290 (2.13)	-50820 (-8.49)	11850 (1.98)

Table 2. Trends in the Southern Hemisphere

Sector/season	Trend (extent) km^2/dec(%/dec)	Error (extent) km^2/dec (%/dec)	Trend (area) km^2/dec(%/dec)	Error (area) km^2/dec (%/dec)
S. Hemisphere	4420 (0.4)	3890 (0.3)	15750 (1.7)	3240 (0.3)
Weddell Sea	-5095 (-1.2)	3320 (0.8)	-2760 (-0.8)	2800 (0.8)
Indian Ocean	280 (0.1)	1660 (0.9)	1020 (0.7)	1460 (1.0)
West. Pacific	1543 (1.2)	1490 (1.2)	4450 (5.0)	1170 (1.3)
Ross Sea	20050 (7.0)	2750 (1.0)	20550 (8.7)	2320 (1.0)
Bell./Amundsen	-12360 (-8.1)	3280 (1.4)	-7510 (-6.5)	1764 (1.5)
Winter	8300 (0.52)	8890 (0.56)	19740 (1.47)	8330 (0.62)
Spring	-1380 (-0.08)	9510 (0.54)	11390 (0.78)	9680 (0.66)
Summer	-11800 (-1.78)	11750 (1.77)	924 (0.21)	8740 (1.95)
Autumn	23340 (3.20)	12360 (1.70)	30720 (5.46)	12220 (1.99)
Maximum	5260 (0.28)	10320 (0.54)	19150 (1.20)	9380 (0.59)
Minimum	-11400 (-3.58)	8994 (2.82)	-7532 (-3.76)	6350 (3.17)

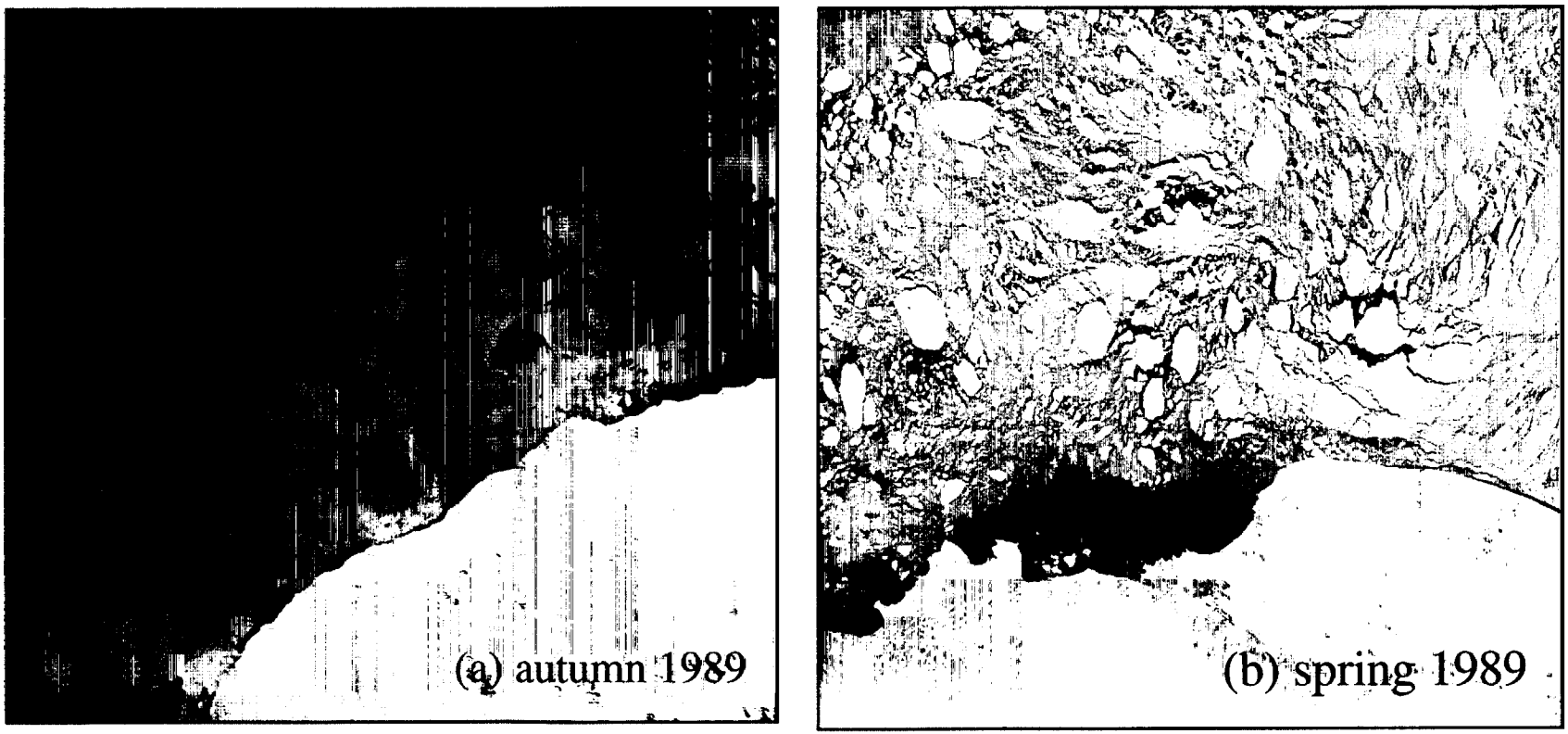

Figure 1

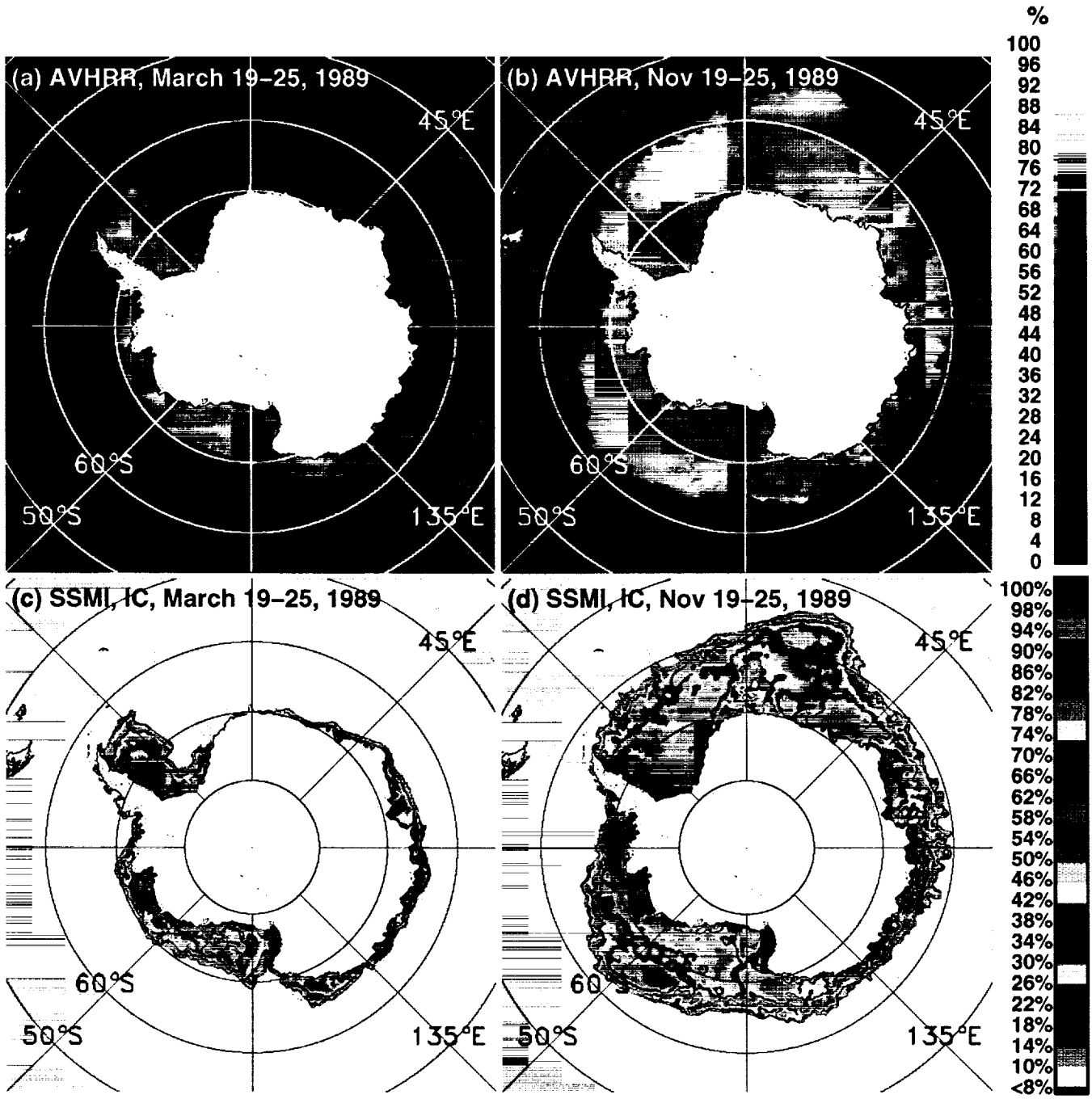
(a) AVHRR, March 19–25, 1989
45°E
60°S
50°S
135°E
(b) AVHRR, Nov 19–25, 1989
45°E
60°S
50°S
135°E
%
100
96
92
88
84
80
76
72
68
64
60
56
52
48
44
40
36
32
28
24
20
16
12
8
4
0
(c) SSMI, IC, March 19–25, 1989
45°E
60°S
50°S
135°E
(d) SSMI, IC, Nov 19–25, 1989
45°E
60°S
50°S
135°E
100%
98%
94%
90%
86%
82%
78%
74%
70%
66%
62%
58%
54%
50%
46%
42%
38%
34%
30%
26%
22%
18%
14%
10%
<8%

Figure 2

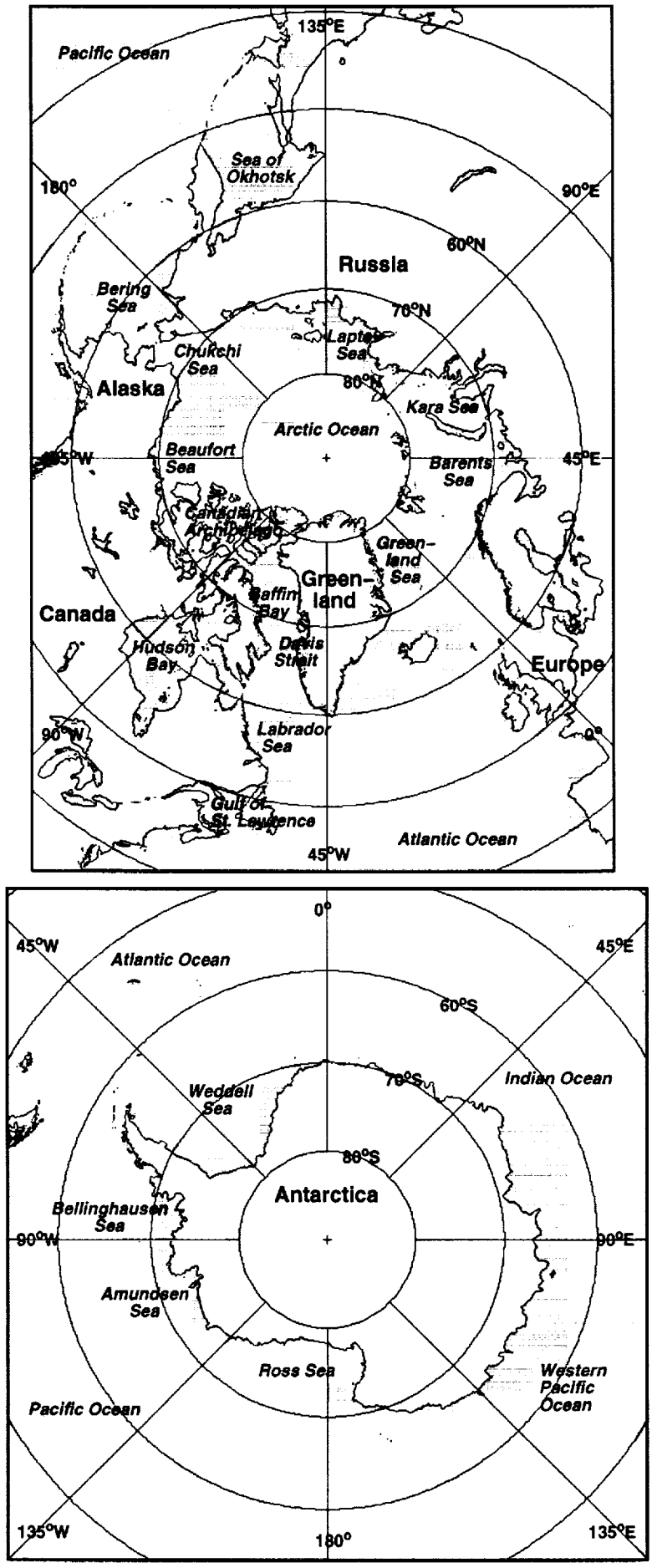
135°E
Pacific Ocean
Sea of Okhotsk
180°
90°E
60°N
Russia
Bering Sea
70°N
Laptev Sea
Chukchi Sea
Alaska
80°N
Kara Sea
Arctic Ocean
Beaufort Sea
45°W
45°E
Barents Sea
Canadian Archipelago
Green-land Sea
Green-land
Baffin Bay
Canada
Davis Strait
Hudson Bay
Europe
90°W
Labrador Sea
0°
Gulf of St. Lawrence
Atlantic Ocean
45°W
0°
45°W
Atlantic Ocean
45°E
60°S
Weddell Sea
70°S
Indian Ocean
80°S
Antarctica
Bellinghausen Sea
90°W
90°E
Amundsen Sea
Ross Sea
Western Pacific Ocean
Pacific Ocean
135°W
180°
135°E

Figure 3

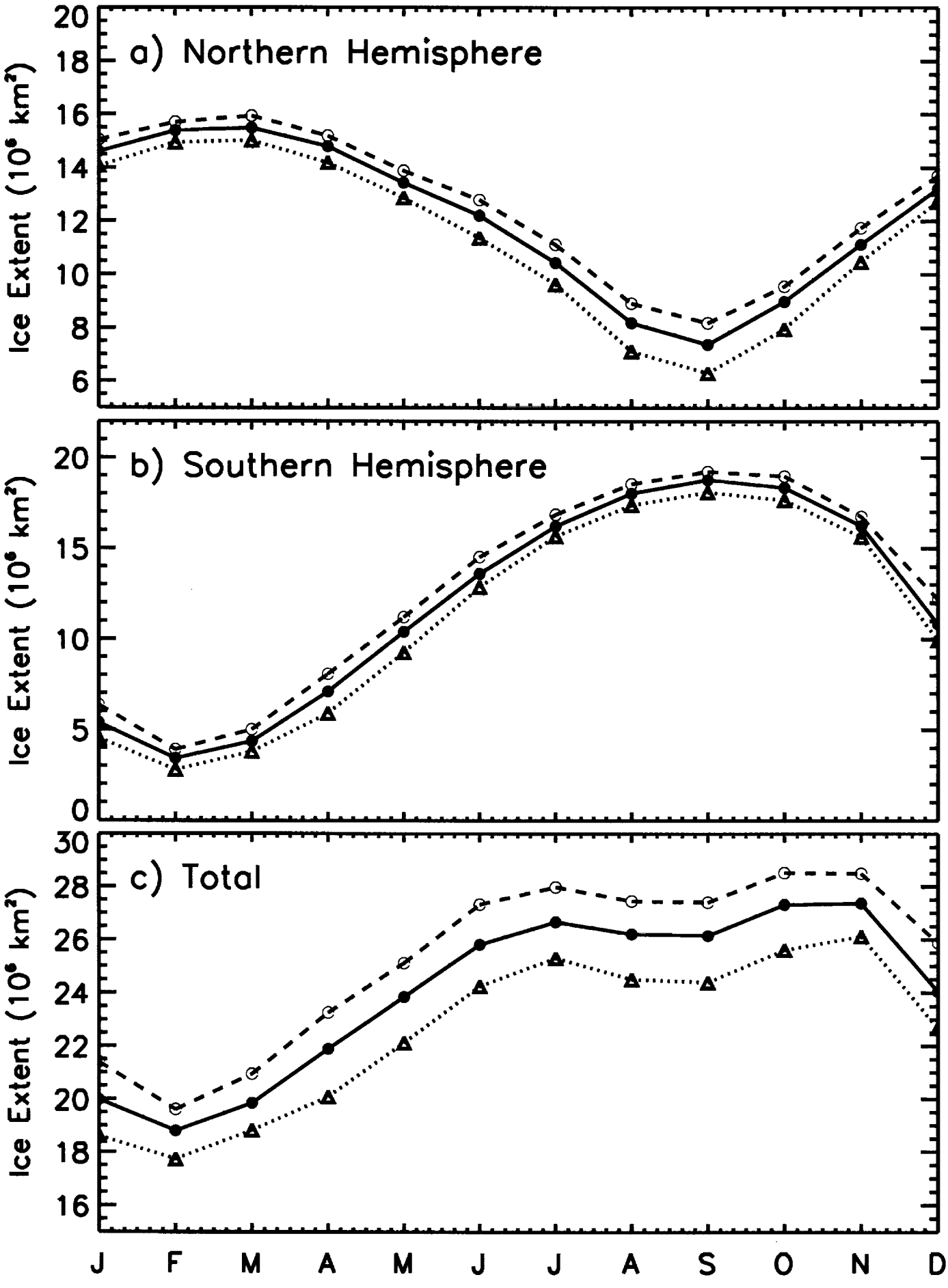
a) Northern Hemisphere
b) Southern Hemisphere
c) Total
Ice Extent (10^6 km^2)
20
18
16
14
12
10
8
6
15
5
0
30
28
26
24
22
20
18
16
J
F
M
A
M
J
J
A
S
O
N
D

Figure 4

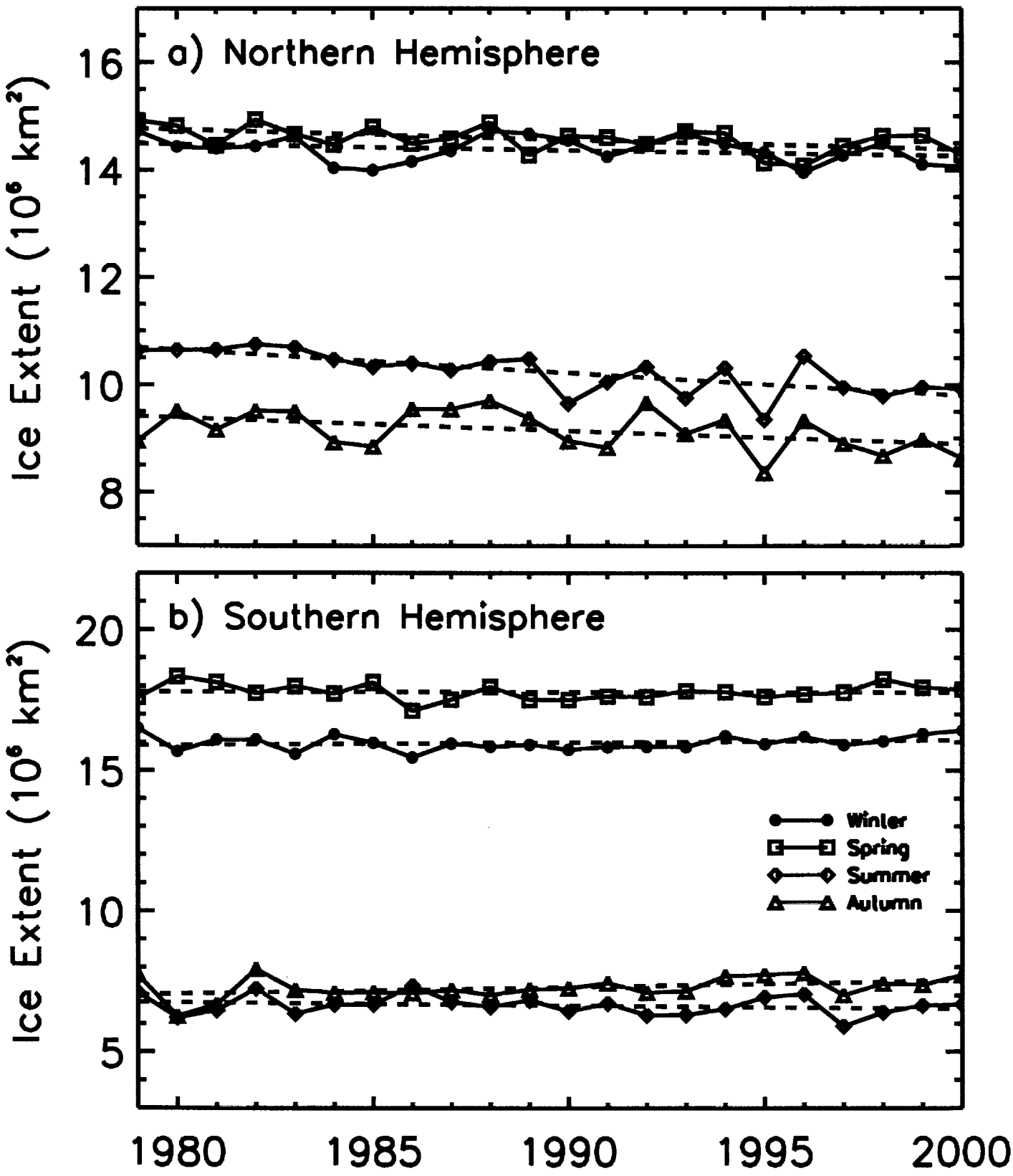
a) Northern Hemisphere
b) Southern Hemisphere
Ice Extent (10^6 km^2)
16
14
12
10
8
20
15
10
5
1980
1985
1990
1995
2000
Winter
Spring
Summer
Autumn

Figure 5

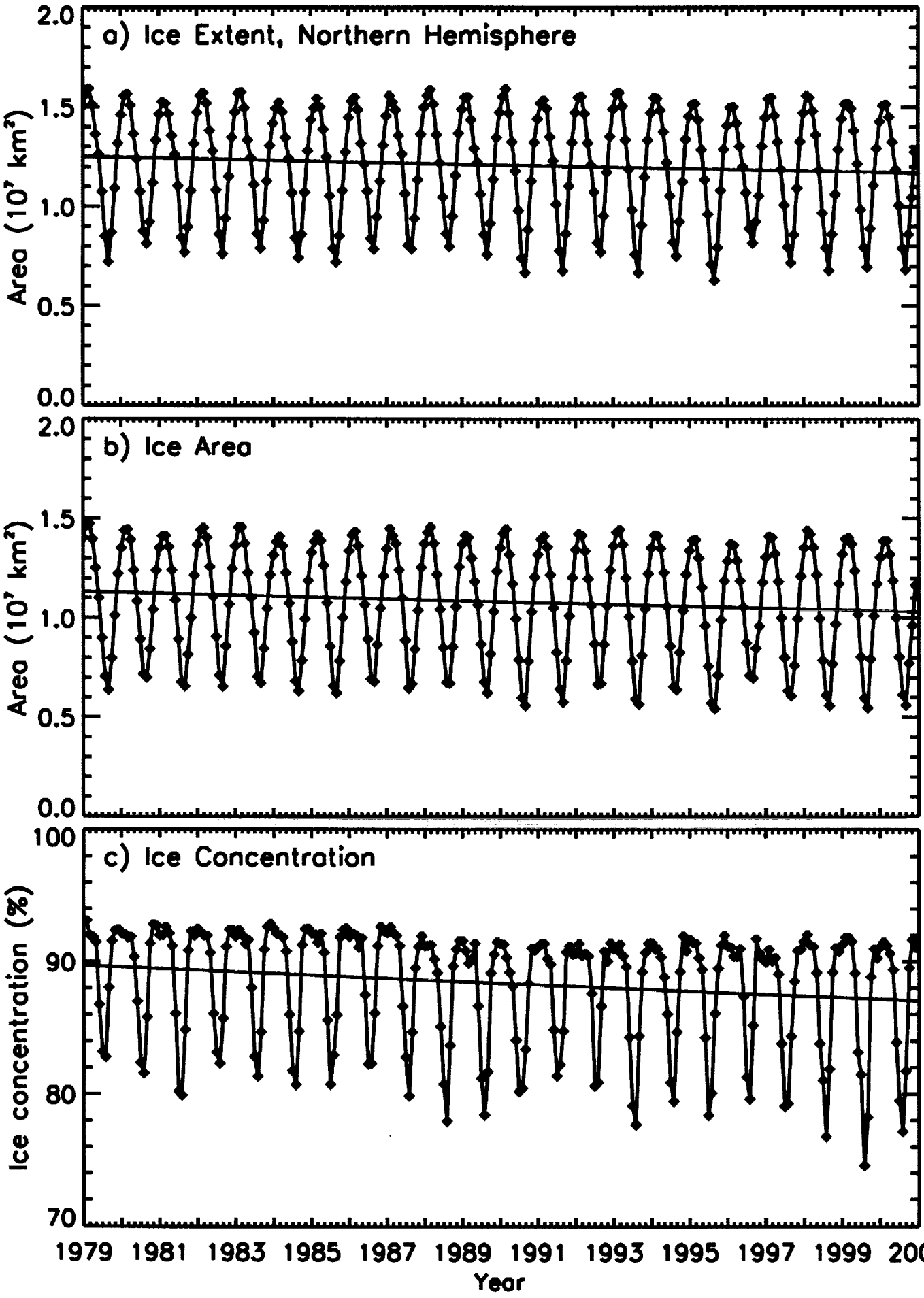
a) Ice Extent, Northern Hemisphere
Area (10⁷ km²)
2.0
1.5
1.0
0.5
0.0
b) Ice Area
Area (10⁷ km²)
2.0
1.5
1.0
0.5
0.0
c) Ice Concentration
Ice concentration (%)
100
90
80
70
1979 1981 1983 1985 1987 1989 1991 1993 1995 1997 1999 2001
Year

Figure 6

Yearly Ice Concentration Anomalies (August–July)

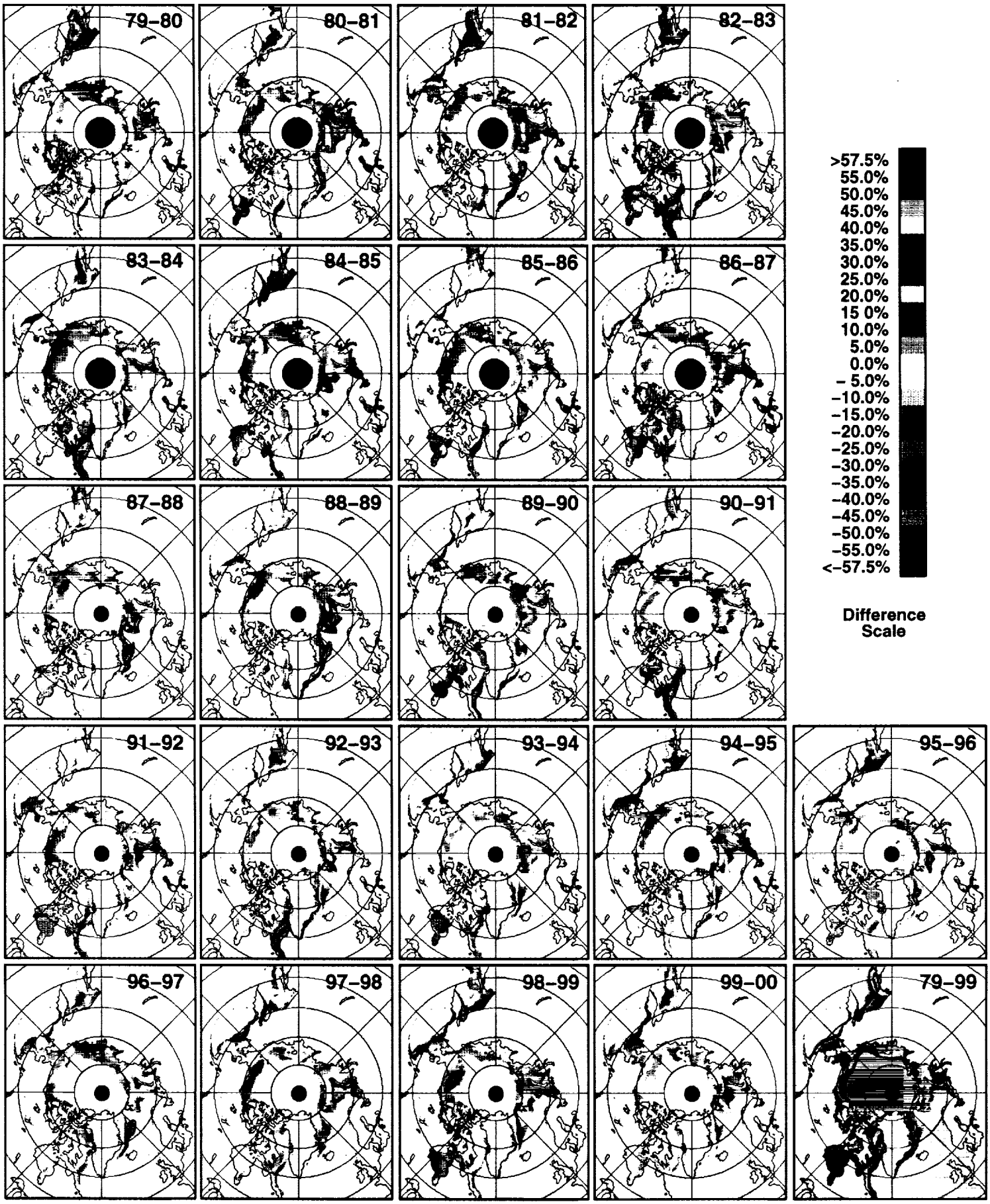

Figure 7

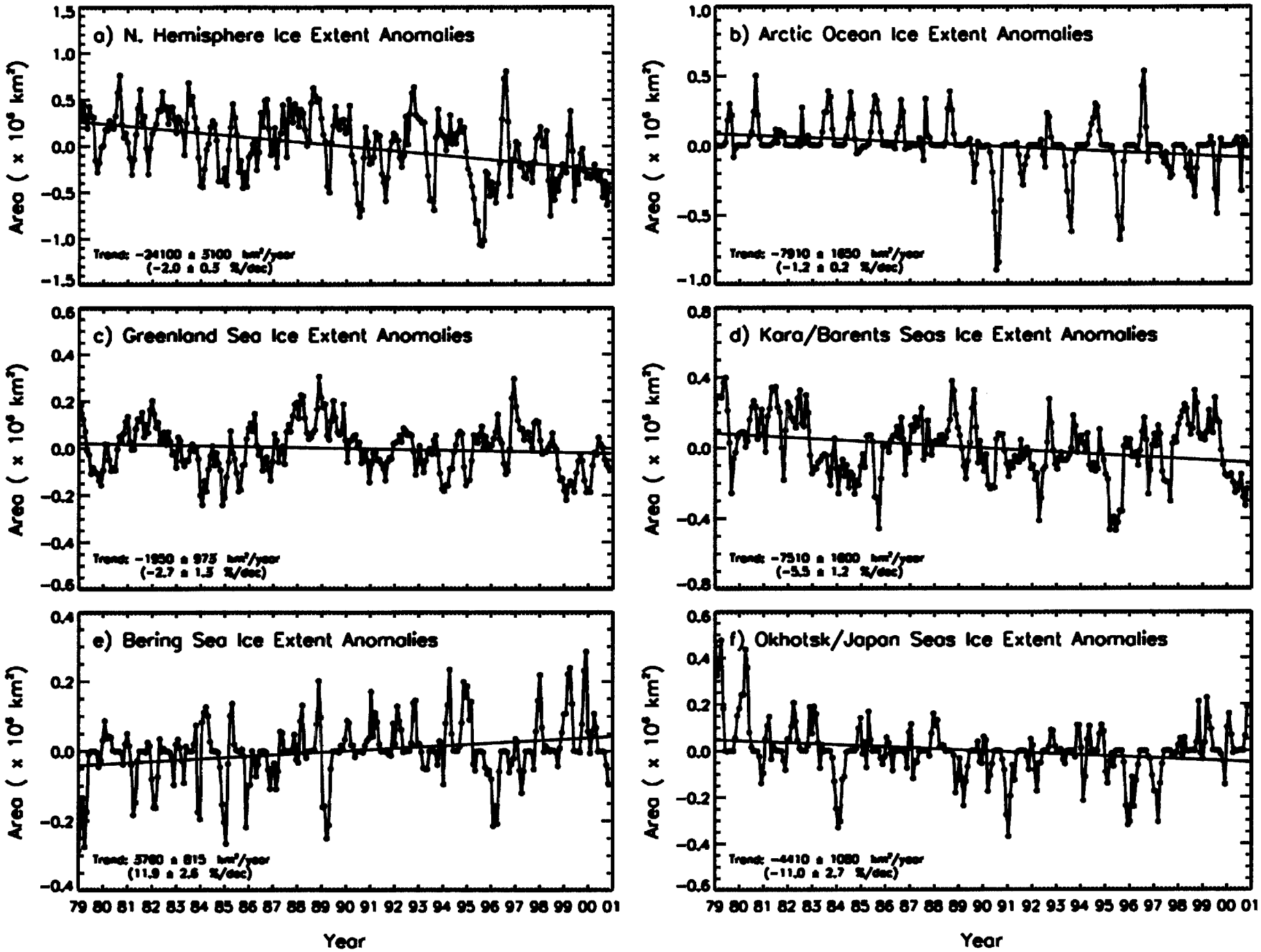
a) N. Hemisphere Ice Extent Anomalies
Trend: -24100 ± 5100 km²/year
(-2.0 ± 0.5 %/dec)
b) Arctic Ocean Ice Extent Anomalies
Trend: -7910 ± 1850 km²/year
(-1.2 ± 0.2 %/dec)
c) Greenland Sea Ice Extent Anomalies
Trend: -1950 ± 975 km²/year
(-2.7 ± 1.3 %/dec)
d) Kara/Barents Seas Ice Extent Anomalies
Trend: -7510 ± 1800 km²/year
(-5.5 ± 1.2 %/dec)
e) Bering Sea Ice Extent Anomalies
Trend: 5780 ± 815 km²/year
(11.9 ± 2.6 %/dec)
f) Okhotsk/Japan Seas Ice Extent Anomalies
Trend: -4410 ± 1080 km²/year
(-11.0 ± 2.7 %/dec)
Area (x 10⁶ km²)
79 80 81 82 83 84 85 86 87 88 89 90 91 92 93 94 95 96 97 98 99 00 01
Year

Figure 8

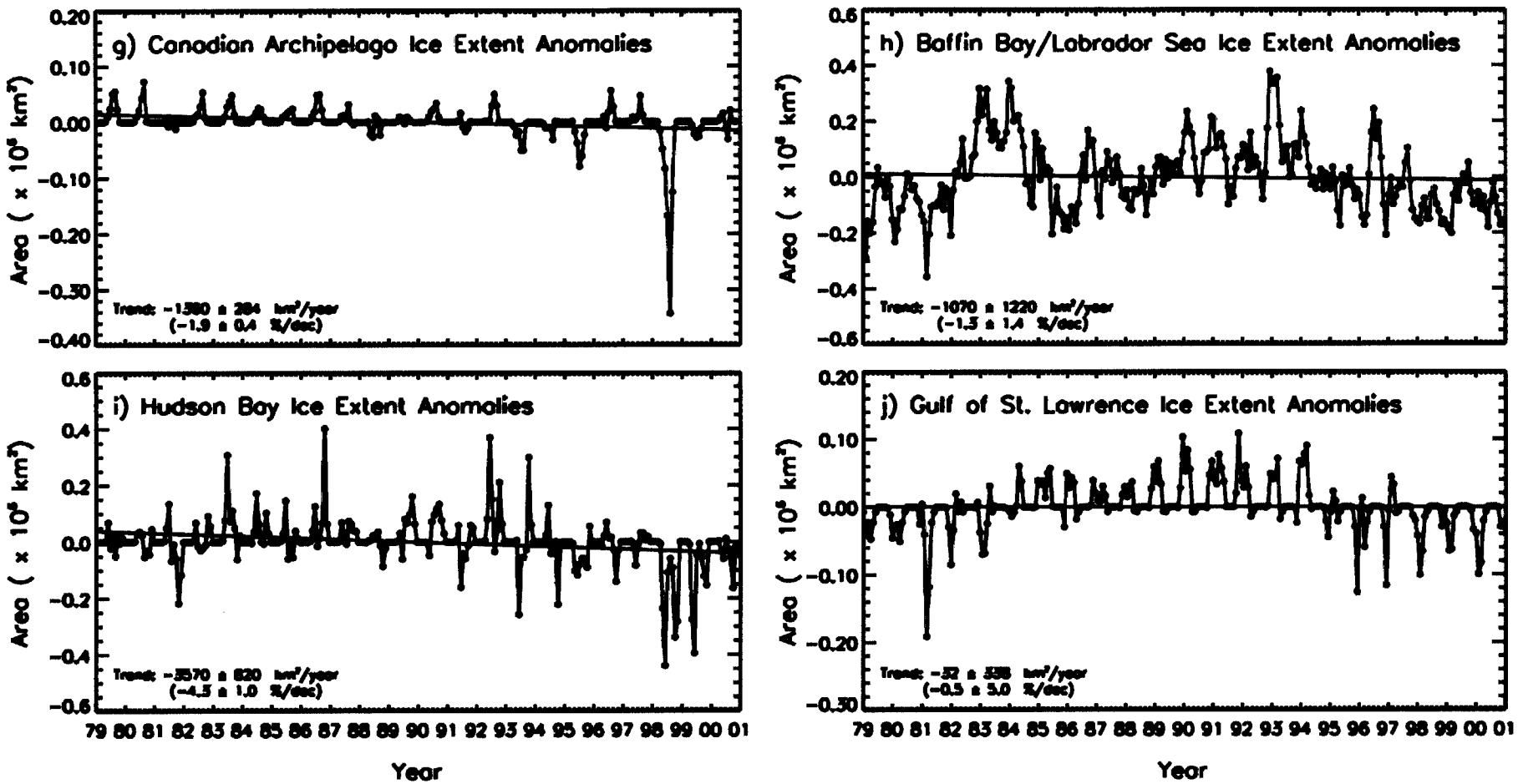
g) Canadian Archipelago Ice Extent Anomalies
Trend: -1380 ± 284 km²/year
(-1.9 ± 0.4 %/dec)
h) Baffin Bay/Labrador Sea Ice Extent Anomalies
Trend: -1070 ± 1220 km²/year
(-1.5 ± 1.4 %/dec)
i) Hudson Bay Ice Extent Anomalies
Trend: -3570 ± 820 km²/year
(-4.5 ± 1.0 %/dec)
j) Gulf of St. Lawrence Ice Extent Anomalies
Trend: -32 ± 338 km²/year
(-0.5 ± 5.0 %/dec)
Area (x 10⁶ km²)
79 80 81 82 83 84 85 86 87 88 89 90 91 92 93 94 95 96 97 98 99 00 01
Year

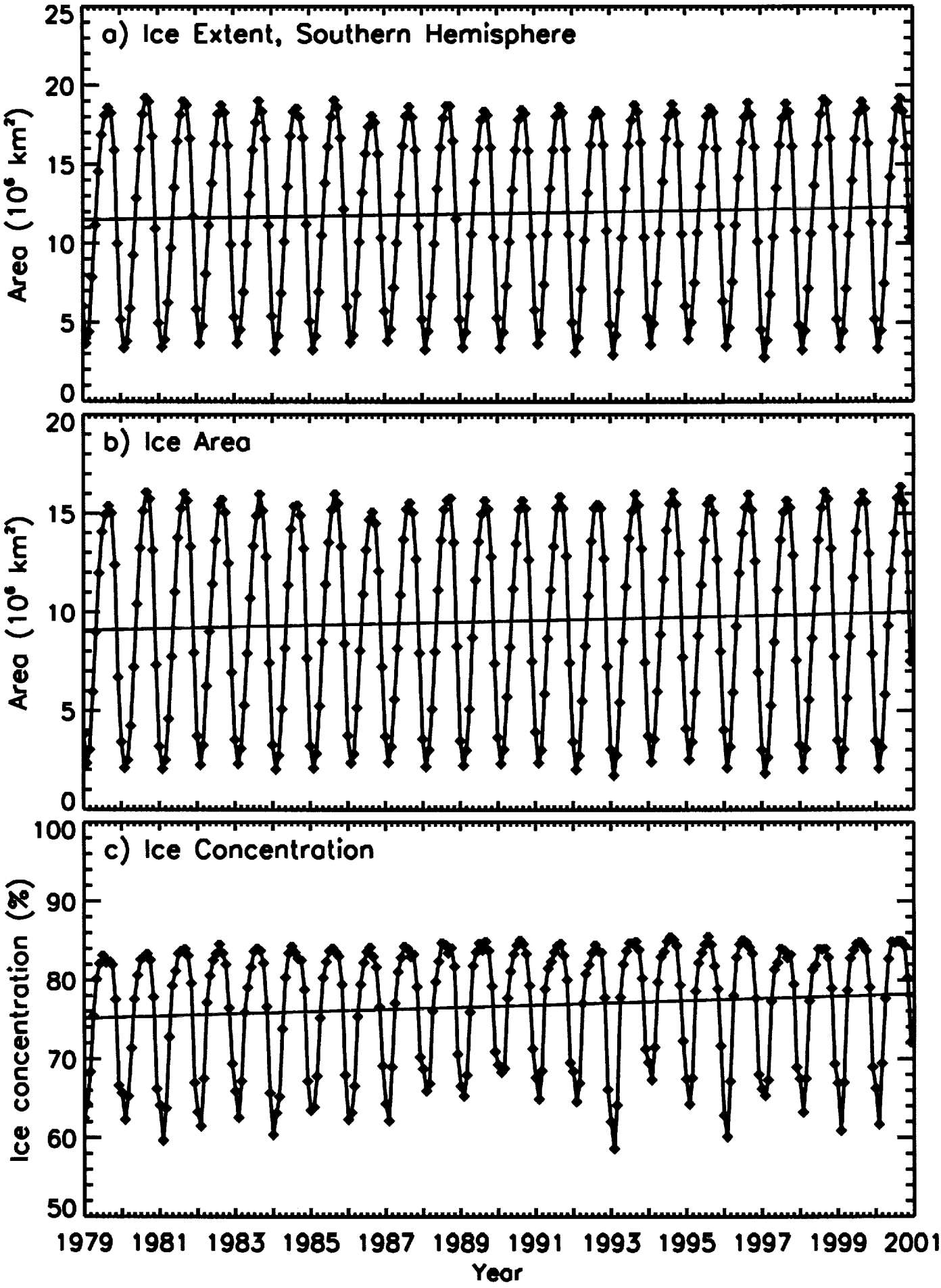
a) Ice Extent, Southern Hemisphere
Area (10^6 km^2)
25
20
15
10
5
0
b) Ice Area
Area (10^6 km^2)
20
15
10
5
0
c) Ice Concentration
Ice concentration (%)
100
90
80
70
60
50
1979 1981 1983 1985 1987 1989 1991 1993 1995 1997 1999 2001
Year

Figure 9

Yearly Ice Concentration Anomalies

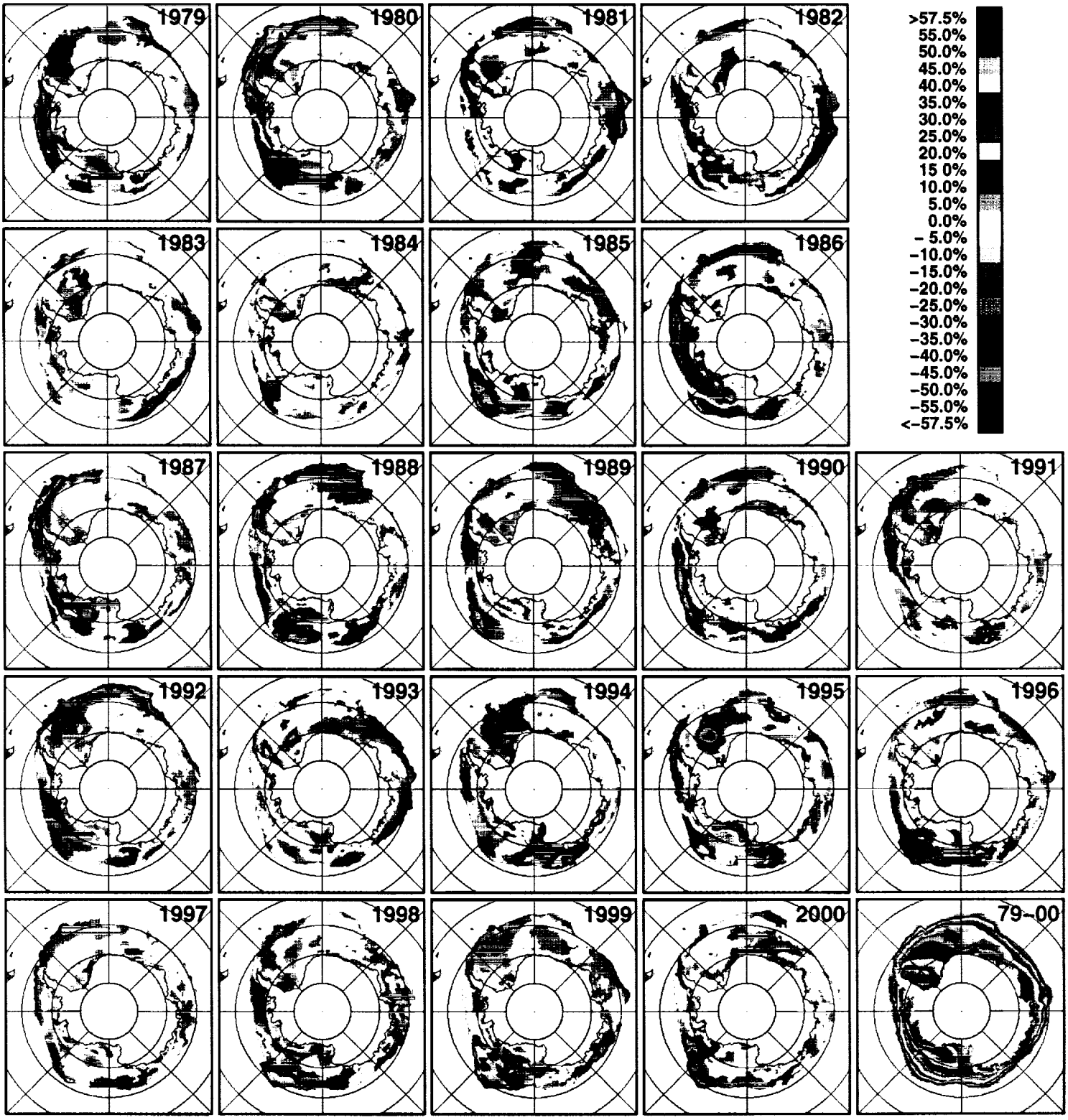

Figure 10

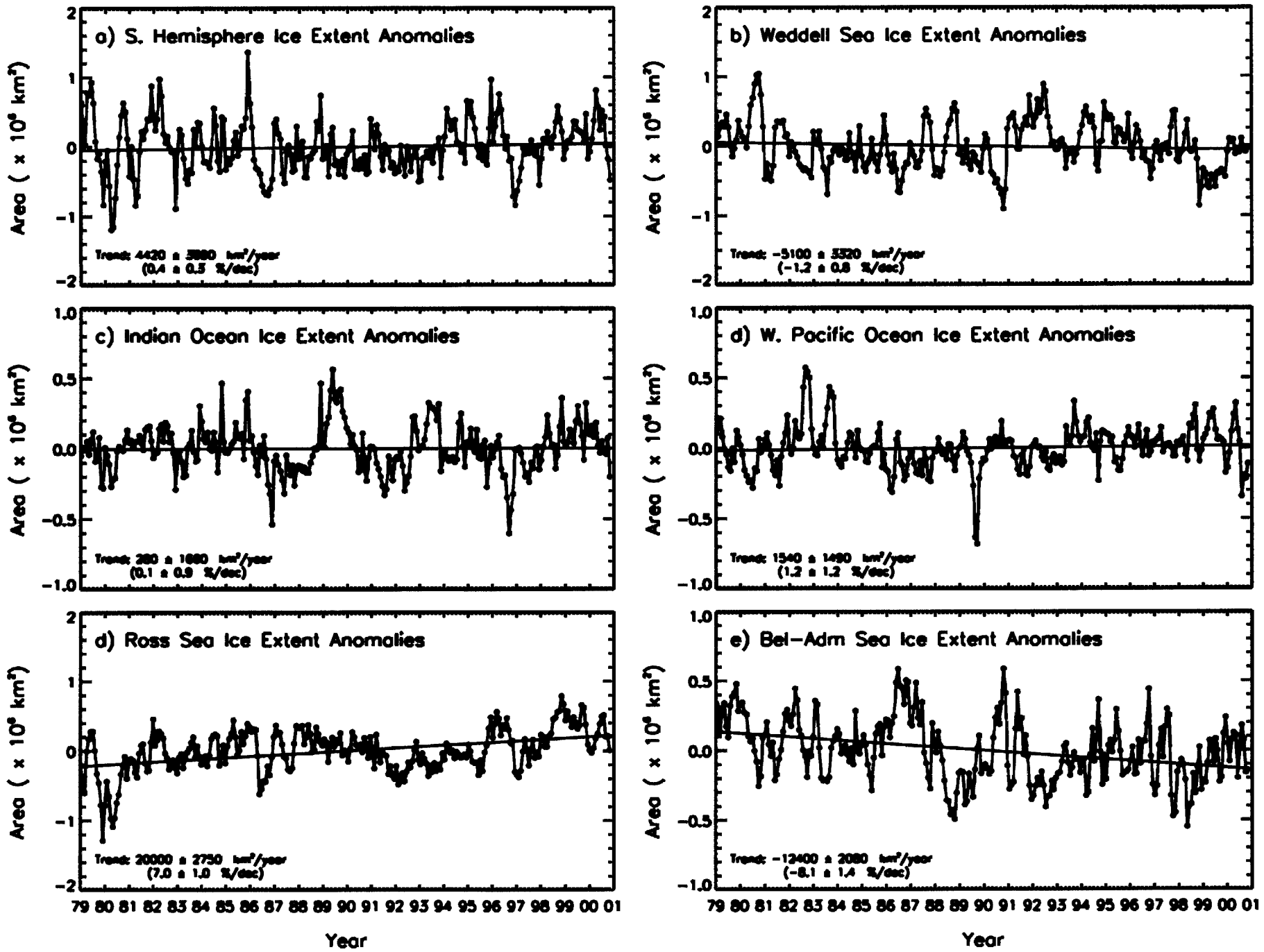
a) S. Hemisphere Ice Extent Anomalies
Trend: 4420 ± 3880 km²/year
(0.4 ± 0.5 %/dec)
b) Weddell Sea Ice Extent Anomalies
Trend: -5100 ± 3320 km²/year
(-1.2 ± 0.8 %/dec)
c) Indian Ocean Ice Extent Anomalies
Trend: 280 ± 1680 km²/year
(0.1 ± 0.9 %/dec)
d) W. Pacific Ocean Ice Extent Anomalies
Trend: 1540 ± 1490 km²/year
(1.2 ± 1.2 %/dec)
d) Ross Sea Ice Extent Anomalies
Trend: 20000 ± 2750 km²/year
(7.0 ± 1.0 %/dec)
e) Bel-Adm Sea Ice Extent Anomalies
Trend: -12400 ± 2080 km²/year
(-8.1 ± 1.4 %/dec)
Area (x 10⁶ km²)
79 80 81 82 83 84 85 86 87 88 89 90 91 92 93 94 95 96 97 98 99 00 01
Year

Figure 11

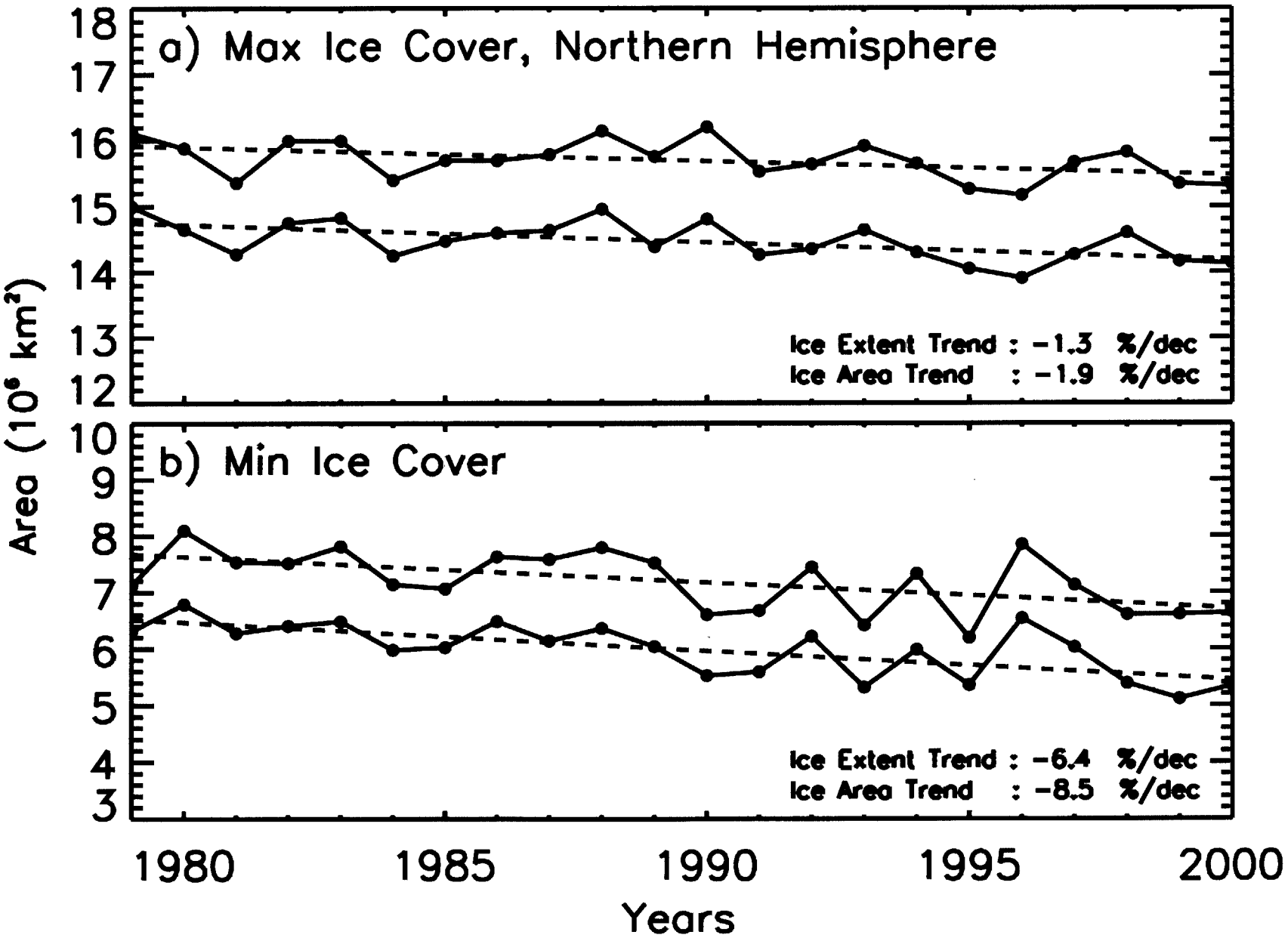
a) Max Ice Cover, Northern Hemisphere
Ice Extent Trend : -1.3 %/dec
Ice Area Trend : -1.9 %/dec
b) Min Ice Cover
Ice Extent Trend : -6.4 %/dec
Ice Area Trend : -8.5 %/dec
Area (10^6 km^2)
Years
18
17
16
15
14
13
12
10
9
8
7
6
5
4
3
1980
1985
1990
1995
2000

Fig. 12

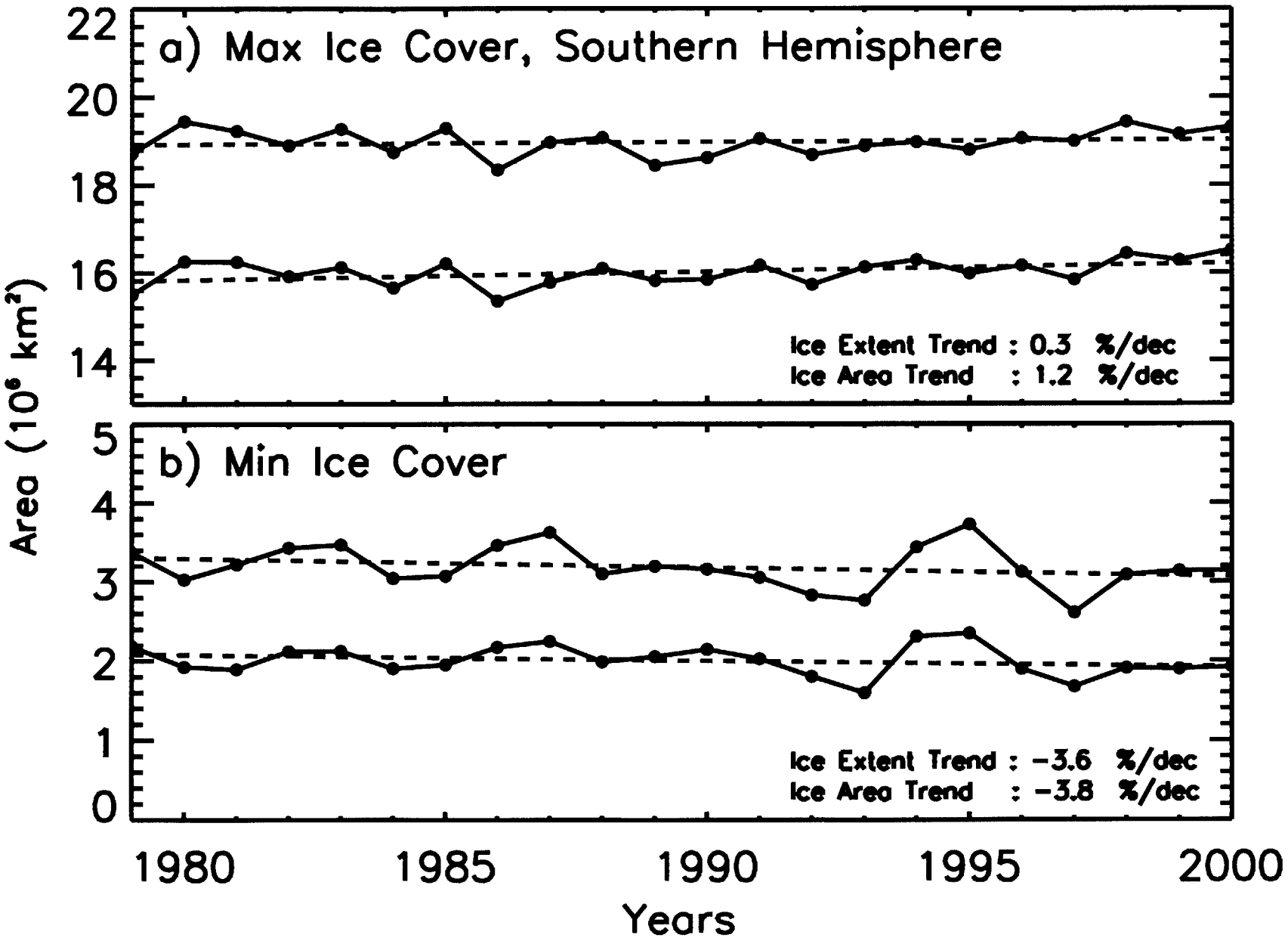
a) Max Ice Cover, Southern Hemisphere
Ice Extent Trend : 0.3 %/dec
Ice Area Trend : 1.2 %/dec
b) Min Ice Cover
Ice Extent Trend : −3.6 %/dec
Ice Area Trend : −3.8 %/dec
Area (10^6 km^2)
Years
22
20
18
16
14
5
4
3
2
1
0
1980
1985
1990
1995
2000

Fig. 13

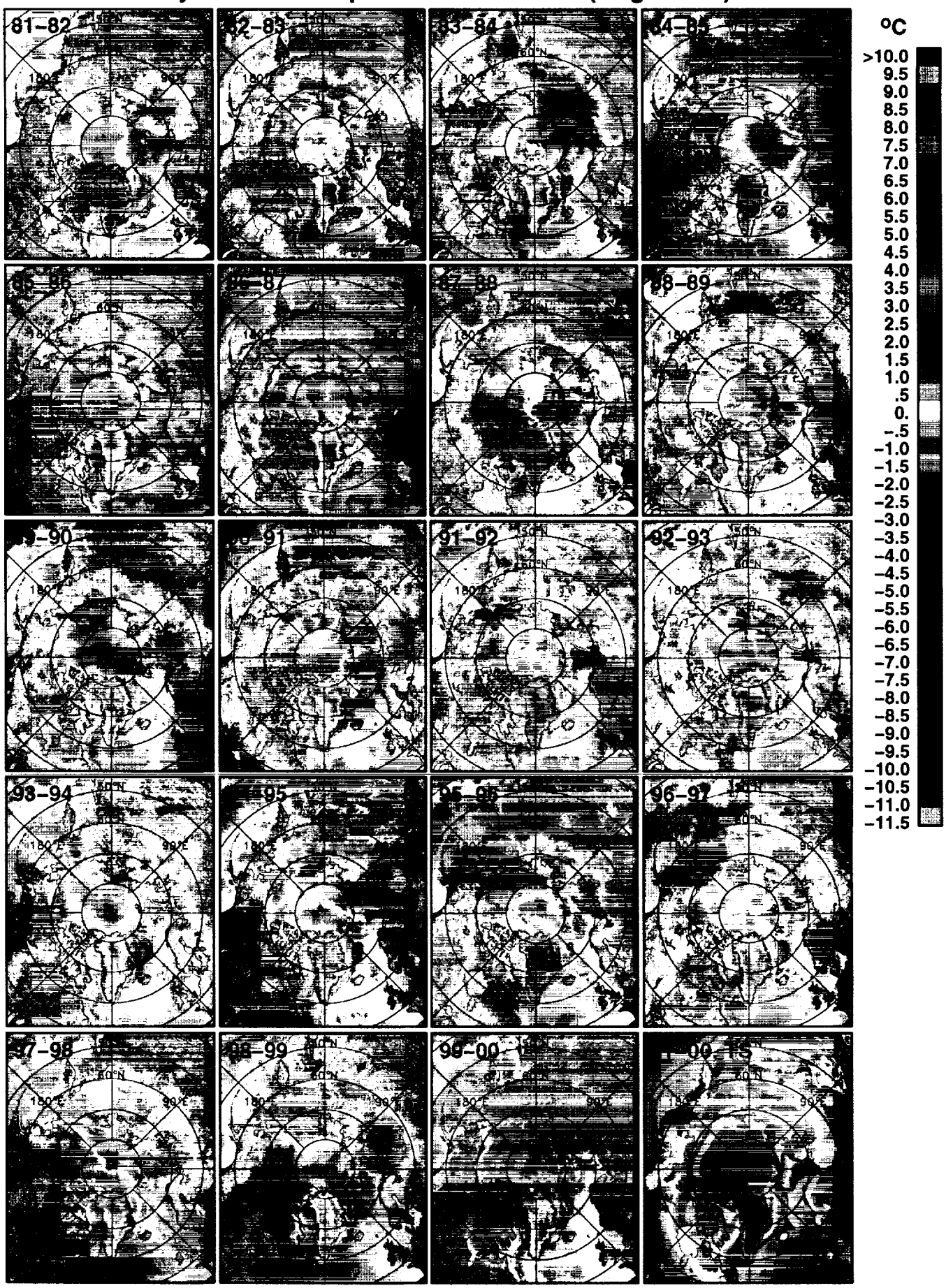
Yearly Surface Temperature Anomalies (Aug. – Jul.)
81–82
82–83
83–84
84–85
85–86
86–87
87–88
88–89
89–90
90–91
91–92
92–93
93–94
94–95
95–96
96–97
97–98
98–99
99–00
°C
>10.0
9.5
9.0
8.5
8.0
7.5
7.0
6.5
6.0
5.5
5.0
4.5
4.0
3.5
3.0
2.5
2.0
1.5
1.0
.5
0.
-.5
-1.0
-1.5
-2.0
-2.5
-3.0
-3.5
-4.0
-4.5
-5.0
-5.5
-6.0
-6.5
-7.0
-7.5
-8.0
-8.5
-9.0
-9.5
-10.0
-10.5
-11.0
-11.5

Figure 14

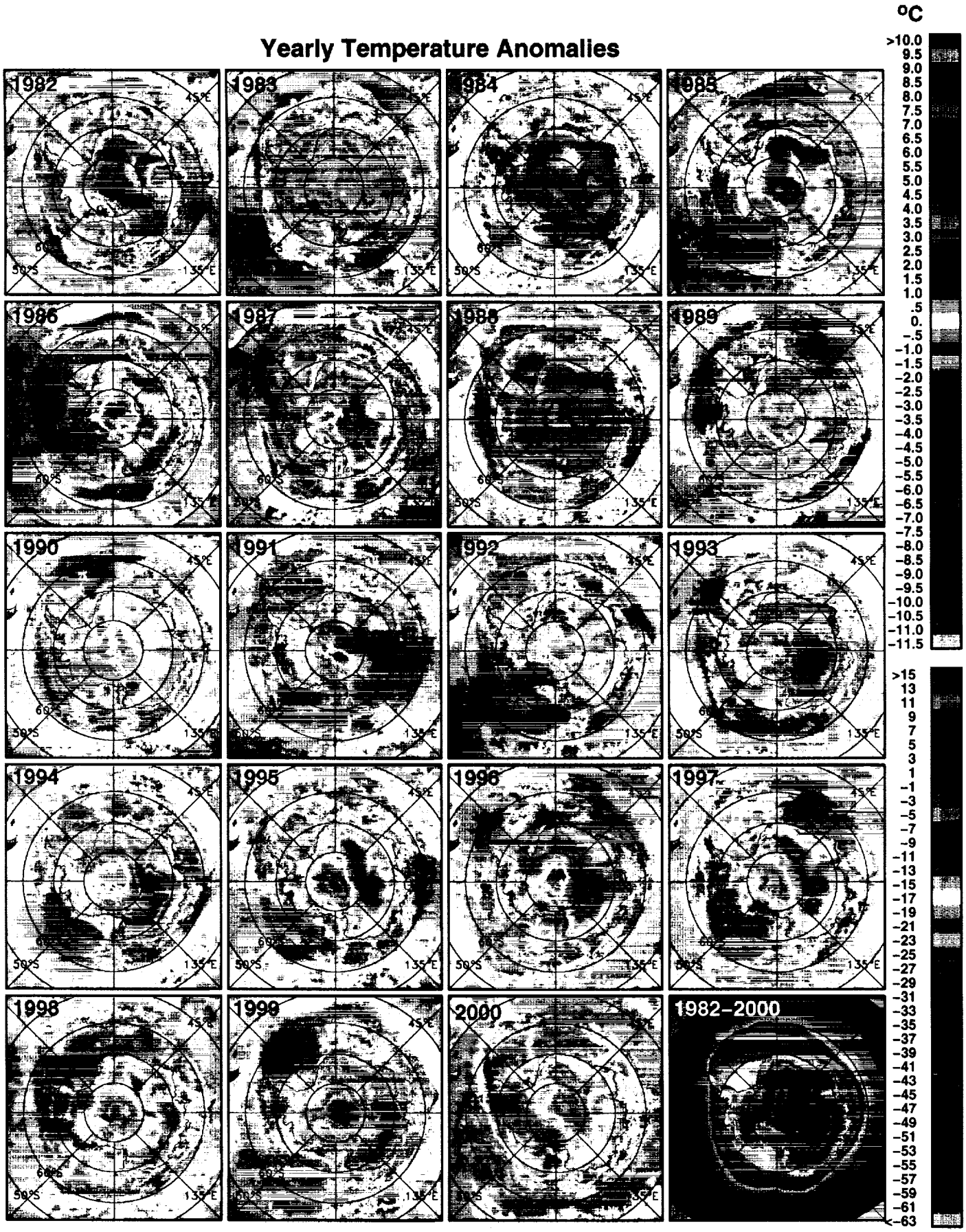
Yearly Temperature Anomalies
°C
>10.0
9.5
9.0
8.5
8.0
7.5
7.0
6.5
6.0
5.5
5.0
4.5
4.0
3.5
3.0
2.5
2.0
1.5
1.0
.5
0.
-.5
-1.0
-1.5
-2.0
-2.5
-3.0
-3.5
-4.0
-4.5
-5.0
-5.5
-6.0
-6.5
-7.0
-7.5
-8.0
-8.5
-9.0
-9.5
-10.0
-10.5
-11.0
-11.5
>15
13
11
9
7
5
3
1
-1
-3
-5
-7
-9
-11
-13
-15
-17
-19
-21
-23
-25
-27
-29
-31
-33
-35
-37
-39
-41
-43
-45
-47
-49
-51
-53
-55
-57
-59
-61
-63
1982
1983
1984
1985
1986
1987
1988
1989
1990
1991
1992
1993
1994
1995
1996
1997
1998
1999
2000
1982-2000

Figure 15

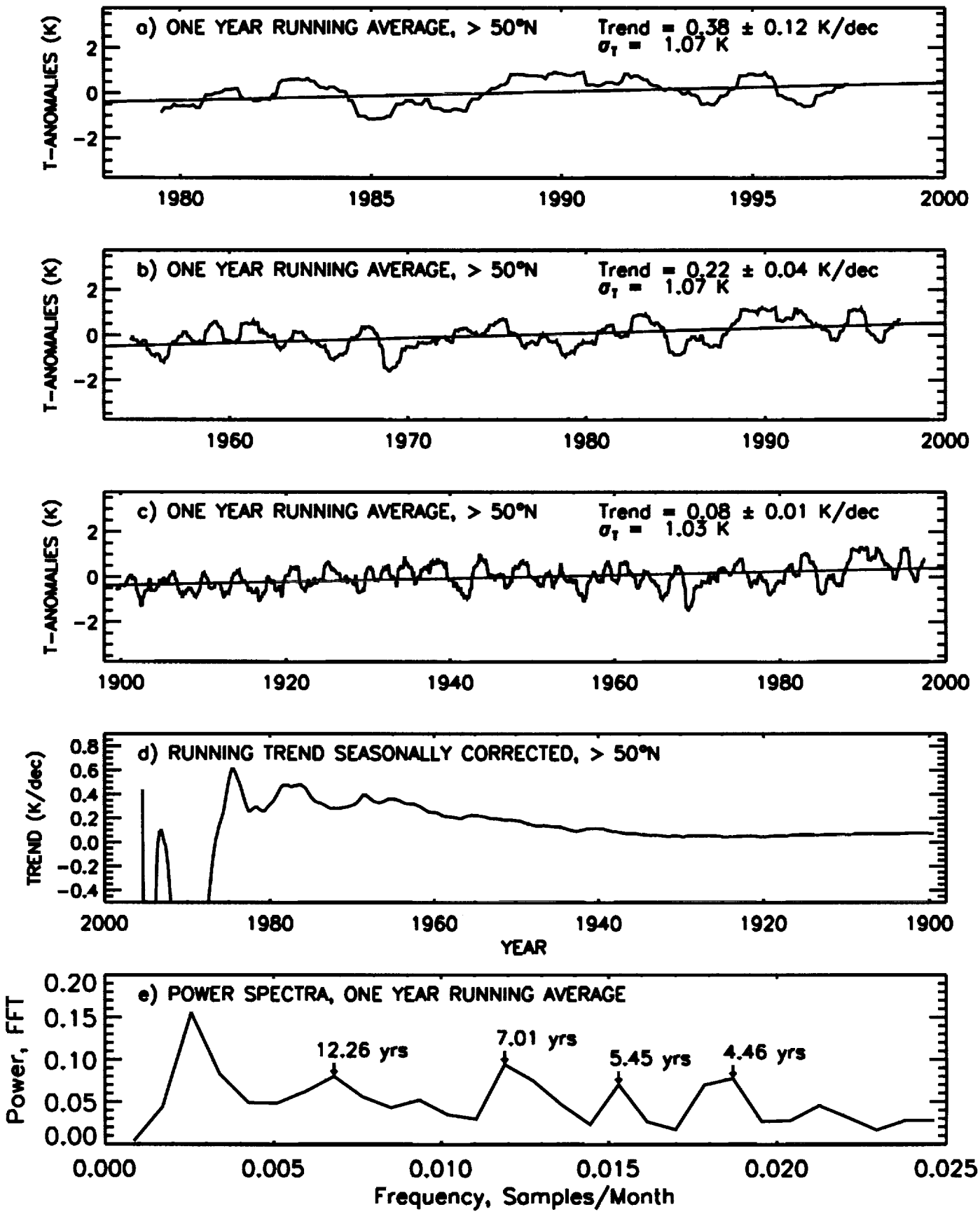
a) ONE YEAR RUNNING AVERAGE, > 50°N
Trend = 0.38 ± 0.12 K/dec
σT = 1.07 K
T-ANOMALIES (K)
b) ONE YEAR RUNNING AVERAGE, > 50°N
Trend = 0.22 ± 0.04 K/dec
σT = 1.07 K
T-ANOMALIES (K)
c) ONE YEAR RUNNING AVERAGE, > 50°N
Trend = 0.08 ± 0.01 K/dec
σT = 1.03 K
T-ANOMALIES (K)
d) RUNNING TREND SEASONALLY CORRECTED, > 50°N
TREND (K/dec)
YEAR
e) POWER SPECTRA, ONE YEAR RUNNING AVERAGE
12.26 yrs
7.01 yrs
5.45 yrs
4.46 yrs
Power, FFT
Frequency, Samples/Month

Figure 16

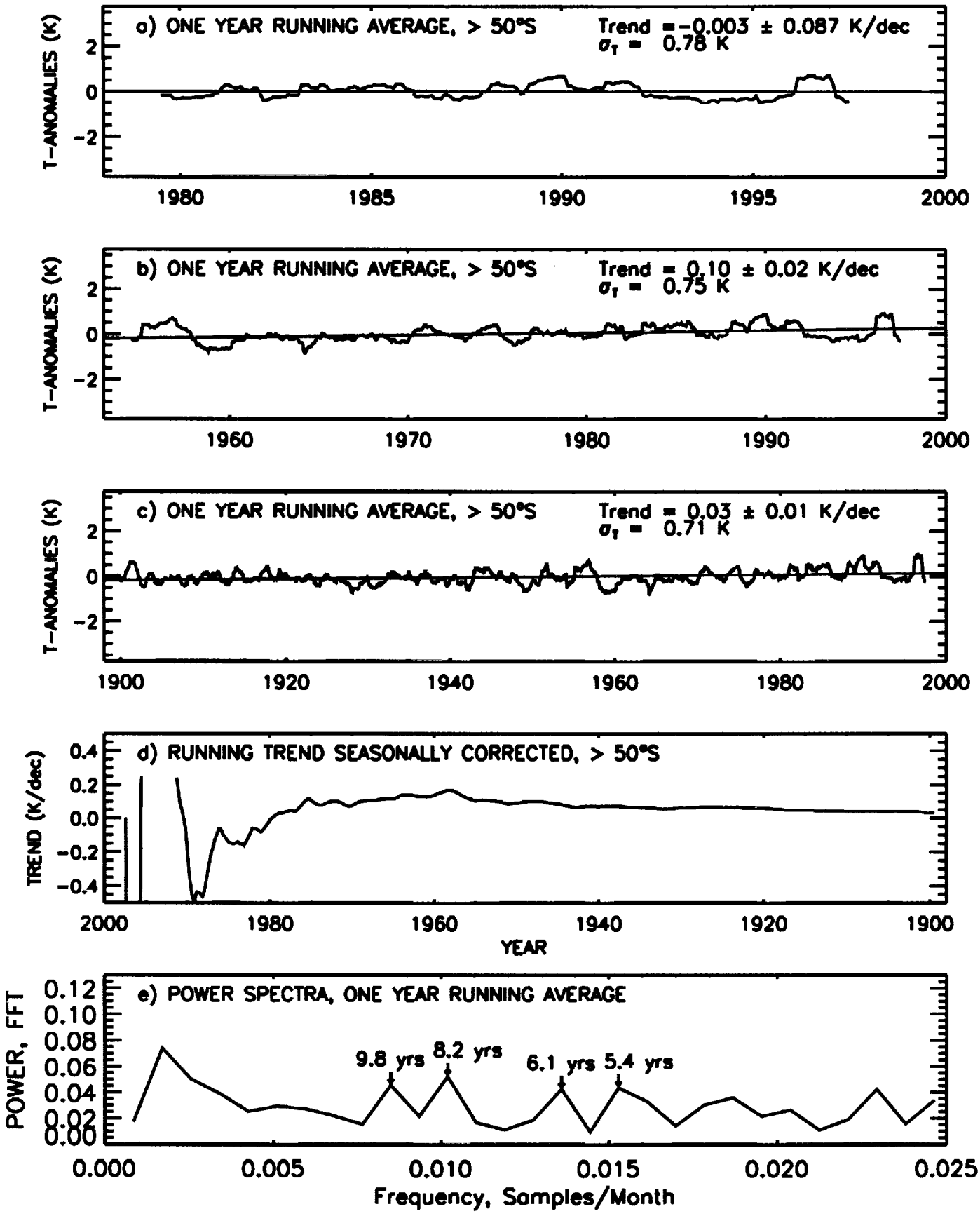
a) ONE YEAR RUNNING AVERAGE, > 50°S
Trend = -0.003 ± 0.087 K/dec
σT = 0.78 K
T-ANOMALIES (K)
2
0
-2
1980
1985
1990
1995
2000
b) ONE YEAR RUNNING AVERAGE, > 50°S
Trend = 0.10 ± 0.02 K/dec
σT = 0.75 K
T-ANOMALIES (K)
2
0
-2
1960
1970
1980
1990
2000
c) ONE YEAR RUNNING AVERAGE, > 50°S
Trend = 0.03 ± 0.01 K/dec
σT = 0.71 K
T-ANOMALIES (K)
2
0
-2
1900
1920
1940
1960
1980
2000
d) RUNNING TREND SEASONALLY CORRECTED, > 50°S
TREND (K/dec)
0.4
0.2
0.0
-0.2
-0.4
2000
1980
1960
1940
1920
1900
YEAR
e) POWER SPECTRA, ONE YEAR RUNNING AVERAGE
POWER, FFT
0.12
0.10
0.08
0.06
0.04
0.02
0.00
9.8 yrs
8.2 yrs
6.1 yrs
5.4 yrs
0.000
0.005
0.010
0.015
0.020
0.025
Frequency, Samples/Month

Figure 17

Large Scale Characteristics and Variability of the Global Sea Ice Cover

Josefino C. Comiso
Laboratory for Hydrospheric Processes, Code 971
NASA Goddard Space Flight Center
Greenbelt, MD 20771

Popular Summary:

Climate change warming signals that may be caused by greenhouse gases are expected to be amplified in the polar regions because of feedback effects associated with the high albedo of snow and ice. This is a book chapter for a general scientific reading public that provides an exhaustive overview of the characteristics and state of the global sea ice cover as inferred from two decades of satellite data. Large seasonal fluctuations in the ice extent and area are apparent in both hemispheres with abnormally large winter extents usually followed by abnormally depleted summer ice cover. Yearly anomaly maps of ice concentrations show a predominance of positive values in the 1980s and negative values in the 1990s. Surface temperature anomaly data derived from 19 years of thermal infrared AVHRR data also show similar patterns but with opposite signs. Regression analysis results show that the ice extent and ice area have been declining at the rate of $-2.0 \pm 0.5\%$ and $-3.1 \pm 0.3\%$ per decade, respectively, in the Northern Hemisphere but there are regions like the Bering Sea with positive trends. Somewhat intriguing, however, is that the perennial sea ice cover has been on a decline at a much faster rate than the entire hemisphere, i.e., $6.7 \pm 2.4\%$ and 8.3 ± 2.4 % per decade for ice extent and ice area, respectively, while surface temperatures during end of summer over the same region have been increasing at the rate of $0.9 \pm 0.6\%$ per decade. The perennial sea ice cover consists mainly of thick multiyear ice floes, and its persistent decline would mean profound changes in the Arctic Ocean including its productivity and its ecosystem. In the Antarctic, large year to year anomalies in the ice cover are observed but they follow a pattern of alternating positive and negative anomalies around the continent. Similar patterns are observed in the yearly surface ice temperature anomaly maps that together with the ice data show consistency with a propagating Antarctic Circumpolar Wave (ACW) that circles around Antarctica. Unlike the Arctic, the trend in the Antarctic ice cover is slightly positive at 0.4 ± 0.3 % per decade and is consistent with surface air temperature trends in the continent during the last 2 decades. However, the ice cover in the Bellingshausen/Amundsen Seas sector has been declining considerably at -8.1 ± 1.4 % per decade while the adjacent Ross Sea sector has been gaining ice at almost the same (but positive) rate of 7.0 ± 1.0 % per decade. The historical record of surface temperatures from meteorological stations is used as a proxy for ice extent and results show that during the last century, the trend for the Arctic is less negative while for the Antarctic it is slightly negative. Spectral analysis of this data also show some periodic cycles in both hemispheres that may have some connections with ENSO and the Arctic Oscillation.